

OFDM SYSTEM AND PAPR REDUCTION TECHNIQUES IN OFDM SYSTEM

A MAJOR PROJECT REPORT

Submitted by

G. SURESH

Roll No: B081195

K. MOUNIKA

Roll No: B081447

in partial fulfillment of major project for the award of degree

of

BACHELOR OF TECHNOLOGY

in

ELECTRONICS & COMMUNICATIONS ENGINEERING



RGUKT – Basar Campus

Rajiv Gandhi University Of Knowledge Technologies

Basar, Adilabad (Dist), Andhra Pradesh

May 2014



RGUKT-Basar

Rajiv Gandhi University of Knowledge Technologies (RGUKT)

(Approved by AICTE(Permanent Institute ID.1-854082611))

Basar, Mudhole (Mandal), Adilabad (Dist.), Andhra Pradesh-504107

CERTIFICATE

This is to certified that the project report entitled “**OFDM SYSTEM AND PAPR REDUCTION TECHNIQUES IN OFDM SYSTEM**” is the bonafide work carried out and submitted by **G.Suresh (B081195), K.Mounika (B081447)** to the Department of Electronics & Communications Engineering, Rajiv Gandhi University of Knowledge Technologies (RGUKT) - Basar, in practical fulfillment for the award of **Bachelor of Technology (ELECTRONICS & COMMUNICATION ENGINEERING)** during the academic year 2013-2014. To the best of my knowledge this project work free from plagiarism. In case found to be plagiarized we, students will take the responsibility.

Supervisor

Mr. A. Ch. Madhusudana Rao

M.Tech.(IIT Madras)

Dept. of Electronics & Communication Engineering

Rajiv Gandhi University of Knowledge Technologies, Basar

DECLARATION

We hereby declare that the work embodied in this report has been carried out by us under the supervision of **Mr. A.Ch.Madhusudhana Rao** in the department of Electronics & Communciation Engineering, Rajiv Gandhi University of Knowledge Technologies, Basar and has not been sbmitted to any other University, Information derived from the published and unpublished work of others has been acknowledged and a list of reference is given.

Place:

Date:

Gurugubilli Suresh (B081195)

Kamani Mounika (B081447)

ACKNOWLEDGEMENT

The successful completion of our project is indeed practically incomplete without mentioning of all those encouraging people who genuinely supported and encouraged us throughout the project. There are several people who deserve more than a written acknowledgement of exemplary help.

First of all we would like to thank our parents and almighty for their constant support and encouragement. Through this acknowledgment, we express our sincere gratitude to **Mr. Raj Kumar** Honorable Vice Chancellor of RGUKT, **Mr. G. Srinivas Sagar** Central Coordinator of Electronics & Communication Engineering, RGUKT, **Mr. M. Laxman** Head of Department of Electronics & Communication, RGUKT-Basar, **Mr. Chakravarthi Jada**, In-Charge of ECE Project works, RGUKT-Basar for having given us an opportunity to do our Major Project on Communication Systems and have helped us with it and made it a worthwhile experience.

At the very outset we would like to express the deepest appreciation, profound gratitude and deep regards to our guide **Mr. A. Ch. Madhusudhana Rao**, Faculty at RGUKT-Basar, for his exemplary guidance, monitoring and constant encouragement throughout this project. The blessing, help and guidance given by him time to time shall carry us a long way in the journey of life on which we are about to embark.

LIST OF ACRONYMS AND ABBREVIATION

Abbreviation	Definition
A/D	Analog to Digital Conversion
ACI	Adjacent Channel Interference
ADSL	Asymmetric Digital Subscriber Lines
AFC	Adaptive Frequency Correction
AWGN	Additive White Gaussian Noise
BER	Bit Error Rate
BPSK	Binary Phase Shift Keying
CCC	Concentric Circle Constellation
CCDF	Complementary Cumulative Distribution Function
CDF	Cumulative Distribution Function
CF	Crest Factor
CFO	Carrier Frequency Offset
CIR	Carrier to Interference Ratio
CP	Cyclic Prefix
D/A	Digital to Analog Conversion
DAB	Digital Audio Broadcasting
DFT	Discrete Fourier Transform
DQPSK	Differential Quadrature Phase Shift Keying
DVB	Digital Video Broadcasting
ETSI	European Telecommunications Standards Institute
FCC	Federal Communications Commission
FDM	Frequency Division Multiplexing
HDTV	High Definition Television
HiperLAN	High Performance Radio LAN
HPA	High Power Amplifier
i.i.d	Independent and Identically Distributed
IBI	Inter Block Interference
ICI	Inter Carrier Interference
IDFT	Inverse Discrete Fourier Transform
IEEE	Institution of Electrical and Electronics Engineers

IFFT	Inverse Fast Fourier Transform
ISI	Inter symbol Interference
ISM	Industrial Scientific and Medical
LCT	Linear Companding Transform
MATLAB	Matrix Laboratory
MBWA	Mobile Broadband Wireless Access
MCM	Multicarrier Modulations
MIMO	Multiple Input Multiple Output
OFDM	Orthogonal Frequency Division Multiplexing
OFDMA	Orthogonal Frequency Division Multiplexing Access
OOB	Out-of-band
P/S	Parallel to Serial
PAPR	Peak-to-Average Power Ratio
PDF	Probability Distribution Function
PHY	Physical
POCS	Projection onto Convex Sets
PRT	PAPR Reduction Tones
PSD	Power Spectral Density
PSK	Phase Shift Keying
PTS	Partial Transmit Sequence
QAM	Quadrature Amplitude Modulation
QPSK	Quadrature Phase Shift Keying
RF	Radio Frequency
S/P	dSerial to Parallel
SER	Symbol Error rate
SI	Side Information
SLM	Selected Mapping
SNR	Signal to Noise Ratio
TI	Tone Injection
TR	Tone Reservation
VHDSL	Very High-speed Digital Subscriber Lines
VLSI	Very Large Scale Integration
WiMAX	Worldwide Mobility for Wireless Access
WLAN	Wireless Local Area Network

LIST OF SYMBOLS

Symbol	Definition
T	Transmitted symbol duration
N	Number of subcarriers in OFDM system
f_k	kth subcarrier frequency
X_k	Modulated data symbol on kth subcarrier
T_s	OFDM symbol duration
Δf	Frequency separation between two subcarriers
$x(t)$	Continuous time-domain OFDM signal
τ_m	Maximum delay spread of multipath channel
$h(\tau, t)$	Impulse response of multipath fading channel
B_c	Coherence bandwidth of channel
$\{\varphi_k(t)\}_{k=0}^{N-1}$	A set of N orthogonal functions
T_{CP}	Duration of the cyclic prefix
N_{CP}	Number of samples in cyclic prefix
$n(t)$	Additive white Gaussian noise signal
$y(t)$	Continuous time domain OFDM signal at receiver input
$\max_{0 \leq t \leq T_s} [.]$	Maximum value function
P_{av}	Average power of OFDM signal (x(t))
L	Oversampling factor
$x[n]$	nth sample of discrete time domain OFDM signal
$E[.]$	Expectation operator
$x_{BP}(t)$	Bandpass OFDM signal
f_c	Carrier frequency of bandpass OFDM signal
$\text{Re}\{.\}$	Real part operator
$\text{Im}\{.\}$	Imaginary part operator

$\Pr\{x\}$	Probability distribution function of x
$x^c(t)$	OFDM signal after clipping
$\angle x(t)$	phase of $x(t)$
M	μ -law companding function parameter
$x_{\mu c}[n]$	μ -law companded discrete time domain OFDM signal
$x_{\mu e}[n]$	OFDM signal after expander
$\text{sgn}(\cdot)$	Signum function
$r[n]$	OFDM signal received at the expander input
x_m	m th partial transmit sequence
$b(m)$	phase rotation factor for m th sub-block
X_m	m th sub-block
x'	Minimum PAPR OFDM signal after applying PTS
B	Set of phase factors
S	Number of partitions
W	Number of phase factors in phase set
$\phi_{b(m)}$	Optimum phase factor for m th sub-block
U	Number of alternative sequences in SLM-OFDM system
X^{TR}	Frequency domain OFDM signal after applying TR
$x^{\text{TR}}[n]$	Discrete time domain OFDM signal after applying TR

LIST OF FIGURES

Figure 2.1: Multicarrier Modulation	8
Figure 2.2: Principle of multicarrier demodulation	9
Figure 2.3: Time domain representation of the signal waveform to show orthogonality among the subcarriers	11
Figure 2.4: The time dispersion and Corresponding received signals timing	12
Figure 2.5: Cyclic Prefix	13
Figure 2.6: Time dispersion and corresponding received signal using cyclic prefix insertion	13
Figure 2.7: OFDM modulator	14
Figure 2.8: OFDM demodulator	15
Figure 2.9: Construction of OFDM with 5 subcarriers	
Figure 2.9(a): Time domain representation of all subcarriers	16
Figure 2.9(b): Frequency domain representation of subcarriers	16
Figure 2.9(c): Overall sum of subcarriers (Time domain)	17
Figure 2.9(d): Overall combined frequency response of subcarriers	17
Figure 2.10: OFDM system	18
Figure 3.1: Square root of PAPR for an OFDM signal with 16 subcarrier having same initial phase	22
Figure 3.2: CCDF of PAPR for $N=64,128,256,512$	23
Figure 3.3: CCDF of PAPR for different modulation techniques	24
Figure 4.1: PDF of real part of original and μ -law companded OFDM signal amplitude	28
Figure 4.2: Comparison of PAPR performance of normal and μ -law companded OFDM signal	29
Figure 4.3: BER performance comparison of Normal OFDM and μ -law companding	29
Figure 4.5: PAPR performance comparison of SLM-OFDM system for various values of U	31
Figure 4.6: Block diagram of conventional PTS-OFDM system transmitter	33
Figure 4.7: Comparison of PAPR performance of PTS-OFDM with $W=2$ and 4	34
Figure 4.8: Expanded 16-QAM constellation for Tone Injection Technique	36

Figure 6.1: Result obtained from simulation of OFDM code	39
Figure 6.2: Spectrum of above OFDM signal	39
Figure 6.3: CDF graph obtained from Simulation	40
Figure 6.4: The result obtained by simulating Clipping Technique	40
Figure 6.5: The error signal obtained in Clipping	41
Figure 6.6: The result obtained by implementing SLM	41
Figure 6.7: The ofdm signal with minimum PAPR	42
Figure 6.8: The result obtained by implementing tone reservation	43

LIST OF TABLES

Table 4.1: PAPR of all possible combinations of data block using coding scheme for PAPR reduction	37
---	----

ABSTRACT

Orthogonal Frequency Division Multiplexing is a multi carrier modulations technique, which is an efficient high speed data transmission. It is widely used in various wireless communication systems and standards due to its high data rate, high spectral efficiency and robustness to multipath fading channel. World is running towards high data rate transmission for multimedia applications. In single carrier system, the symbol duration decreases with increase in data rate which leads to Inters Symbol Interference.

It is a multicarrier scheme utilizing the parallel data transmission by means of Frequency Division Multiplexing with overlapping subcarriers without interfering. It means dividing a frequency selective fading channel into small orthogonal flat fading channels. "Orthogonality" prevents the demodulators from seeing frequencies other than their own. And each subchannel has low bit rate and with large number of subchannels gives high data rate. So ISI gets reduced due to large symbol duration. Doppler shift and mismatch between transmitter and receiver local oscillator frequencies gives frequency offset. This Carrier Frequency Offset reduces orthogonality between subcarriers which leads to the signal on one subcarrier to depend on another subcarrier which is known as Inter Carrier Interference. It is a challenge for error free demodulation and detection of OFDM symbols.

The major challenge in OFDM is PAPR along with ICI. Here, we are trying to implement the techniques for reducing PAPR as high PAPRs require highly linear amplifiers. The techniques reduce the PAPR at the cost of complexity. The techniques include Clipping, Companding in distortion based techniques and Selected Mapping(SLM), Partial Transmit Sequences(PTS), Tone Reservation, Coding schemes in non-distortion techniques.

CONTENTS

TITLE PAGE	i
CERTIFICATE	ii
DECLARATION	iii
ACKNOWLEDGEMENT	iv
LIST OF ACRONYMS AND ABBREVIATION	v
LIST OF SYMBOLS	vii
LIST OF FIGURES	ix
LIST OF TABLES	x
ABSTRACT	xi
CONTENTS	xii
CHAPTER 1: INTRODUCTION	1
1.1:Background to OFDM	1
1.2:Motivation	3
1.3:Problem Definition	4
1.4:Scope of thesis	4
1.5:Contributions of the Thesis	5
CHAPTER 2: OFDM	6
2.1:Histroy behind OFDM	6
2.2:Multicarrier Modulation	8
2.3:Inter Symbol Interference	9
2.4:Orthogonality	10
2.5:Cyclic Prefix	12
2.6:OFDM Transmitter and Receiver	14
CHAPTER 3: PEAK TO AVERAGE POWER RATIO	19
3.1:PAPR	19
3.1.1:PAPR of Baseband OFDM Signal	20

3.1.2:PAPR of Bandpass OFDM Signal	20
3.1.2:Upperbound of OFDM signal	21
3.2:PDF of OFDM	22
3.3:Complemetary Cumulative Distribution Function	23
CHAPTER 4: PAPR REDUCTION TECHNIQUES	25
4.1:Distrortion Techniques	26
4.1.1:Clipping	26
4.1.2:Comanding	27
4.2:Non-Distortion Techniques	30
4.2.1:Selective Mapping(SLM) Techniques	30
4.2.2:Partial Transmit Method(PTS)	32
4.2.3:Tone Reservation	35
4.2.4:Block Coding Techniques	36
CHAPTER 5: METHODOLOGY ADOPTED	38
5.1:Clipping Method	38
5.2:Selective Mapping	38
5.3:Tone Reservation	38
CHAPTER 6: SIMULATION RESULT	39
6.1:Generation of OFDM signal & Spectrum	39
6.2:Cummulative Distribution Function(CDF)	40
6.3:Clipping Technique	40
6.4:Slective Mapping(SLM) Technique	41
6.5:Tone Reservation	42
CHAPTER 7: CONCLUSIONS AND FUTURE WORK	44
REFERENCES	45
APPENDICES	46

CHAPTER 1

INTRODUCTION

High data-rate is desirable in recent wireless multimedia applications. Traditional single carrier modulation techniques can achieve only limited data rates due to the restrictions imposed by the multipath effect of wireless channel and the receiver complexity. In single carrier systems, as the data-rate in communication system increases, the symbol duration gets reduced. Therefore, the communication systems using single carrier modulation suffer from severe inter-symbol interference (ISI) caused by dispersive-channel impulse response, and thereby need a complex equalization scheme. Orthogonal Frequency Division Multiplexing (OFDM) is a potential candidate to fulfill the requirements of current and next generation wireless communication systems.

1.1 BACKGROUND TO OFDM

OFDM is a special form of multicarrier modulation scheme, which divides the entire frequency selective fading channel into many orthogonal narrowband flat-fading sub channels, in which high-bit-rate data stream is transmitted in parallel over a number of lower data rate subcarriers thereby substantially reducing the ISI due to larger symbol duration. The fundamental principle of OFDM originates from the paper by Chang, and over the years a number of researchers have worked on this technique. Despite its conceptual elegance, its use was initially limited to military systems, such as KINEPLEX, KATHRYN and ANDEFT due to its implementation difficulties. Weinstein and Ebert's proposal to use the Discrete Fourier Transform (DFT) to perform the subcarrier modulation with a single oscillator was a pioneering effort. Ebert, Salz and Schwartz demonstrated the efficacy of Cooley-Tukey fast Fourier transform (FFT) algorithm to further reduce the computational complexity of DFT, thereby making it possible to utilize the OFDM technique in commercial communication systems. Its use in commercial systems started with a number of wire-line standards, which included High bit rate Digital Subscriber Lines (HDSL), Asynchronous Digital Subscriber Lines (ADSL), and Very high speed Digital Subscriber Lines (VDSL), to support a throughput upto 100Mbps. Thereafter, it has been utilized by wireless standards like DAB and WLAN, DVB and WMAN. In WMAN applications, OFDM is considered for the World wide Interoperability for Microwave Access (WiMAX) implementation via standards. OFDM is also being considered for 3GPP

Long term Evolution (LTE) and 3GPP LTE-Advanced. Undoubtedly, OFDM can be a potential air interface candidate for future generation high speed wireless communications systems.

OFDM systems use cyclic prefix insertion to eliminate the effect of ISI and require a simple one-tap equalizer at the receiving end. OFDM brings in unparalleled bandwidth savings, leading to higher spectral efficiency. These properties make OFDM system extremely attractive for high speed wireless applications. In OFDM systems different modulation schemes can be used on individual sub-carriers which are adapted to the transmission conditions on each sub-carrier.

Advantages:

- It is immune to delay spread as symbol duration is much greater than channel delay spread.
- It has resistance to frequency selective channel as each subchannel is flat fading.
- Each subchannel is almost flat fading so it only needs a one tap equalizer to overcome channel effect leads to easy equalization.
- Each subchannel maintain orthogonality with overlapping leads to efficient usage of bandwidth.

Drawbacks in OFDM:

- OFDM signals with their high peak-to-average power ratios (PAPRs) require highly linear amplifiers. Otherwise, performance degradation occurs and out-of-band power requirement will be enhanced.
- OFDM systems are more sensitive to Doppler spread than single-carrier modulated systems.
- Phase noise caused by the imperfections of the transmitter and receiver oscillators degrades the system performance.
- Accurate frequency and time synchronization is required.
- Loss in spectral efficiency due to cyclic-prefix (CP) operation takes place in OFDM systems.

1.2 MOTIVATION

Increasing the spectral efficiency of wireless communication systems is one of the greatest challenges faced by wireless communication engineers. The available bandwidth is scarce and costly, whereas, there is a huge demand for data rate created by increasing number of users and increase in multimedia applications, which require large bandwidth. OFDM, with its spectrally efficient versions like MIMO-OFDM and multiple access versions like OFDMA are under active consideration to fulfill the requirements of present and next generation wireless systems. Large envelope fluctuation in OFDM signal is one of the major drawbacks of OFDM technique. Such fluctuations create difficulties, because practical communication systems are peak-power limited. Envelope peaks require the system to accommodate an instantaneous signal power that is much larger than the signal average power, necessitating either low operating power efficiencies or power amplifier (PA) saturation.

In addition to this, OFDM system requires tight frequency synchronization, in comparison to single carrier systems, due to narrowband subcarriers. Therefore, it is sensitive to a small frequency offset between the transmitted and the received signal. The frequency offset may arise due to Doppler effect or due to mismatch between transmitter and the receiver local oscillator frequencies. The carrier frequency offset (CFO) disturbs the orthogonality between the subcarriers, therefore, the signal on any particular subcarrier will not remain independent of the remaining subcarriers. This phenomenon is known as inter-carrier interference (ICI), which is a big challenge for error-free demodulation and detection of OFDM symbols.

The current implementations of OFDM do not fully exploit its capabilities. There are still several approaches which can be explored to reduce the peak-to-power ratio (PAPR) and ICI of OFDM signal. Therefore, the necessity to reduce the PAPR of standard OFDM signal is a prime motivating factor for this work.

Clipping and filtering is the simplest solution to reduce the PAPR but it achieves the PAPR reduction capability at the cost of BER performance degradation. Existing companding transforms achieve acceptable PAPR reduction capability but they introduce high non-linear distortion, due to which their BER performances degrade. Moreover, both the schemes result in out-of-band radiation and in-band distortion. Improving BER performance using companding based PAPR reduction schemes is a prime motivating factor for our work.

The distortion-less schemes provide PAPR reduction capability at the cost of increased computational complexity. The techniques like Selected Mapping (SLM) and Partial Transmit Sequence (PTS), side information (SI) is required at the receiver to recover the original data signal, which not only causes data- rate loss but also results in severe BER performance

degradation, if SI gets corrupted during transmission. In order to avoid spectral deficiency of these schemes, various SI embedding schemes have been proposed, but in most of them the SI detection capability depends on the available signal-to-noise ratio. Elimination of SI requirement at the receiving end motivates a major part of this work.

ICI cancellation schemes effectively mitigate the effect of ICI but PAPR performance of existing ICI cancellation schemes is either same or worse than that of standard OFDM signal. Therefore, there is a necessity to reduce the PAPR of OFDM signal obtained from ICI cancellation schemes. Hence the need for a joint ICI cancellation and PAPR reduction scheme is another motivating factor for this work.

1.3 PROBLEM DEFINITION

High PAPR and ICI are the two major issues in the implementation of an OFDM system. The thesis aims at exploring and arriving at efficient, low complexity schemes for PAPR reduction in OFDM based systems (without ICI cancellation) of practical use. The first problem addressed in this thesis is the high PAPR of an OFDM signal. We begin by exploring the existing PAPR reduction techniques and to find out their advantages and major limitations for implementing a practical OFDM system. Investigation of efficient PAPR reduction schemes for an OFDM system is thus considered as one of the problem areas explored in this thesis.

Being a multicarrier modulation scheme, OFDM brings all major benefits of a multicarrier scheme but unlike single carrier modulation schemes, it suffers from the problem of ICI performances. As discussed above, the PAPR is an important parameter that must be taken into consideration. Final aim of this thesis is to suggest PAPR reduction in OFDM systems.

1.4 SCOPE OF THE THESIS

The goals met by the thesis are as follows:

- Investigation of clipping technique for PAPR reduction scheme and development of a generalized clipping technique with good PAPR and BER performances.
- Mathematical analysis of error performance of Clipping method for PAPR reduction in OFDM systems.
- Study of SLM based PAPR reduction schemes and development of an efficient SLM based PAPR reduction scheme that does not require side information (SI).
- Exploring the available phase sequence set generation schemes for SLM-OFDM system

and proposing a new phase sequence set generation scheme.

- Exploring the available tone reservation scheme.

These all schemes can be implemented by using MATLAB.

1.5 CONTRIBUTIONS OF THIS THESIS

The OFDM based multiple access schemes have been adopted for downlink communication in 3GPP LTE standards, but not chosen in uplink communication due to high PAPR. In uplink communication, when a mobile terminal has to transmit an OFDM signal, it requires an expensive and bulky high power amplifier, which is difficult to accommodate, due to its cost and size limitation. The mobile terminal is also having a limited computational power and battery life. Therefore, the proposed schemes can be utilized in uplink communication because they provide very good PAPR reduction capability with low computational complexity. The quadrilateral companding transform requires only one additional block at transmitter and receiver to perform companding and decompanding operations respectively.

Day by day operational speed of the wireless communications system is increasing with the rapid advances in VLSI technology. Next-generation high data rate wireless communication systems based on OFDM are under consideration. To provide higher data speeds, RF transceivers in next-generation communications are expected to offer higher RF performance in both transmitting and receiving circuitry, to meet the quality of service requirements. Hence computational complexity is not a limiting factor for highly efficient wireless communication systems. The concentric circle constellation and M-2M mapping for SLM and PTS based PAPR reduction schemes are found to be useful because no additional hardware is required to implement the OFDM system. The number of subcarriers in OFDM based next generation communications systems are increasing day-by-day to cater to the need of high data rate, thereby reducing the subcarrier spacing between two adjacent subcarriers, which makes an OFDM based communication system highly sensitive to a small carrier frequency offset (CFO). In order to mitigate the effect of CFO, an ICI cancellation scheme with good CIR, BER and PAPR performances is required. The PAPR performance of existing ICI cancellation schemes is either same or worse than standard OFDM signal with ICI cancellation.

CHAPTER 2

ORTHOGONAL FREQUENCY DIVISION MULTIPLEXING

The demand for high speed wireless applications and limited RF signals bandwidth is increasing day by day. New applications are emerging, not just in the wired systems, but also in the wireless mobile systems. At present, only low rate data services are available for mobile applications. However, there is a demand for high data rates for multimedia applications. In single carrier system, the symbol duration reduces with an increase in data rate and therefore the effect of Inter symbol Interference (ISI) becomes more severe. ISI, in wireless communication systems, is produced due to the memory of dispersive wireless channels. As a general rule, the effect of ISI on error performance of the system is negligible, as long as the delay spread is significantly shorter than the duration of one transmitted symbol (T). This implies that the symbol rate supported by the communication system is practically limited by ISI. If the data rate exceeds the upper limit of data transmission over the channel, a mechanism must be implemented in order to combat the effects of ISI. Channel equalisation techniques can be used to suppress the echoes caused by the channel. But such equalizers pose difficulties in real-time systems operating at several Mbps speed with compact, low-cost hardware. Multicarrier modulation techniques come to rescue in such situations.

Multicarrier modulation, and especially OFDM, is one of the promising candidates that employ a set of subcarriers in order to transmit the information symbols in parallel over the communication channel. It allows the communication system to transmit the data at a lower rate on multiple subcarriers and the throughput of multicarrier system remains equal to the single carrier system. This allows us to design a system supporting high data rates, while maintaining symbol durations much longer than the channel delay spread, thus simplifying the need for complex channel equalization mechanism and can easily combat the effect of ISI.

2.1 HISTORY BEHIND OFDM

In 1966, the concept of multicarrier communication was first introduced by Chang. He suggested a multicarrier scheme utilizing the parallel data transmission by means of frequency division multiplexing (FDM) with overlapping subcarriers. It was found to be an efficient

scheme for bandwidth utilization and to mitigate the effect of multipath propagation. It also eliminated the requirement of high-speed equalization technique. KINEPLEX, ANDEFT and KATHRYN etc. are the few OFDM based systems utilized by US military systems for high frequency applications. The KINEPLEX system was developed by Collins Radio Company for data transmission at high frequency over multipath fading channel, in this system, 20 tones are modulated by DQPSK without filtering, which resulted in overlapping channels. Initially the implementation of an OFDM system with large number of subcarriers was very complex and expensive because it requires the array of sinusoidal generators and coherent demodulators for parallel operations. In order to avoid the crosstalk between the subcarriers, the system should be free from frequency and timing offsets. In 1971, Weinstein and Ebert suggested a scheme to replace the arrays of sinusoidal generators and coherent demodulators by using IDFT and DFT as modulator and demodulator respectively. In 1979, after evolutionary growth and development in signal processing and VLSI technologies, high speed chips can be built around special-purpose hardware performing the large size Fast Fourier Transform (FFT) (efficient algorithm for DFT) at affordable price. In 1980, Peled and Ruiz introduced the concept of cyclic prefix (CP) to maintain the orthogonality between the subcarriers. Since 1990s, OFDM has been utilized for many broadband communication systems, it includes high-bit-rate digital subscriber lines (HDSL), asymmetric digital subscriber lines (ADSL), very high-speed digital subscriber lines (VHDSL), high definition television (HDTV) terrestrial broadcasting etc. It has also been utilized by many wireless standards like Digital Audio Broadcasting (DAB), Digital Video Broadcasting (DVB). Many standards have been proposed for wireless local area networks (WLANs) operating in ISM band, which are based on spread-spectrum technology. In 1997, first OFDM-based WLAN standard, IEEE 802.11, was released. IEEE 802.11 can support a data rate up to 2 Mbps. Later on, in 1999, IEEE approved an OFDM based standard 802.11a for supporting a data rate up to 54 Mbps. During this period ETSI has also standardized the HiperLAN/2 standard, which has adopted OFDM for their PHY standards. In 2001, the FCC came with some new rules for modulations scheme operating in the 2.4 GHz range, which allow IEEE to extend 802.11b to 802.11g standard. Now a days, it has also been used in WiMAX (IEEE 802.16), and mobile broadband wireless access (MBWA) IEEE 802.10. It is also utilized by 4G wireless communication systems, such as IMT-A. It is also been considered for 3GPP Long Term Evolution, which is under deployment.

2.2 MULTICARRIER MODULATION

Frequency division multiplexing (FDM) extends the concept of single carrier modulation by using multiple subchannels within a given frequency band of a communication channel. The total channel bandwidth is divided among a number of subchannels. One of the major advantages of FDM system is that different subchannels in the band can utilize different modulation scheme and transmit dissimilar data. But FDM requires a guard band between adjacent subchannels to allow their separation with low-cost filters at the receiver. Guard bands degrade the bandwidth efficiency of the FDM system in comparison to single carrier system without multiplexing. Multicarrier modulation is an advanced form of Frequency Division Multiplexing (FDM), where a number of frequency sub-bands called subcarriers are allocated to a user. A simplified block diagram of MCM modulator is shown in Fig. 2.3. The input serial data stream is passed to through a serial-to-parallel converter, which splits the input data stream into a number of parallel subchannels. The data in each of the subchannel is applied to a modulator, such that for N subchannels there are N modulators whose carrier frequencies are $f_0, f_1, \dots, f_k, \dots, f_{N-1}$. These N modulated subcarriers are then combined to give a multicarrier modulated signal.

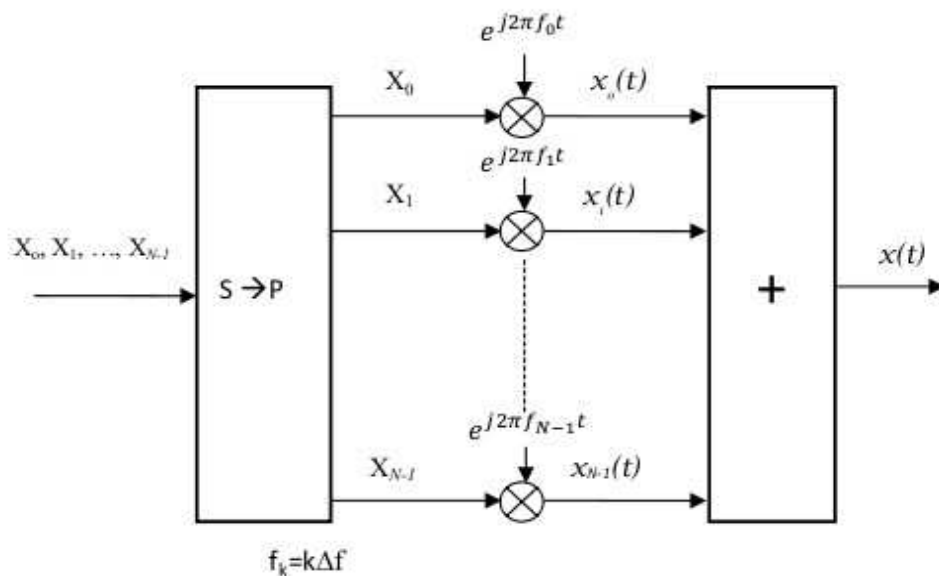


Figure 2.1: Multicarrier Modulation

It illustrates the basic multicarrier demodulator consisting of a bank of correlators, one for each of the subchannel or subcarrier. Under ideal conditions, the local oscillators used to generate the subcarrier frequencies are assumed to be synchronized with corresponding local oscillators used at the transmitter; therefore subcarriers do not cause any interference to each other at the receiver.

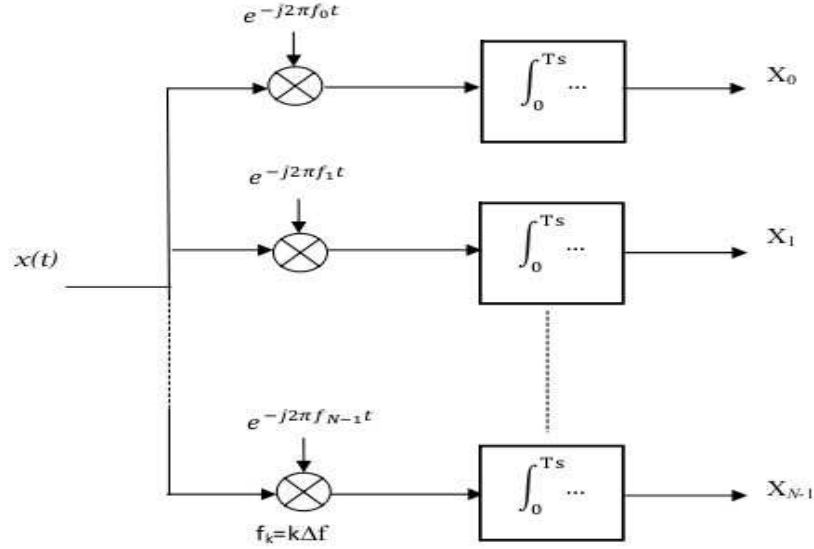


Figure 2.2: Principle of multicarrier demodulation

2.3 Inter Symbol Interference :

The dispersive nature of wireless channel produces the spreading of the modulation symbols in the time domain, which is known as delay spread (τ_m). The effect of the time dispersion is reflected by the ISI phenomenon. A single-carrier system with high data rate is highly affected by ISI problem. Multicarrier modulation has surfaced to mitigate the effect of ISI produced in single carrier systems under the condition $\tau_m > T$. Hence, the main idea is to increase the symbol duration to reduce the effect of ISI. Reducing the effect of ISI yields an easier equalization, which in turn means a simpler reception technique. Multicarrier modulation divides the high rate bit stream into N lower rate substreams, each of which has symbol duration ($T_s = NT$) $\gg \tau_m$, and hence the effect of ISI can be eliminated to a great extent. These individual low data rate substreams are sent over N parallel subcarriers or subchannels, maintaining the total desired data rate of the system.

The above solution can be clarified by considering the following example: Assuming a single-carrier system with total available bandwidth (BT) of 1MHz, we transmit the data at symbol duration of 1 μ s. Consider a typical outdoor scenario where the maximum delay spread can be as high as 10 μ s, so in the worst-case scenario, at least 10 consecutive symbols will be affected by the ISI due to the delay spread. A scenario for comparing the single carrier modulation scheme with multicarrier modulation is illustrated below.

Comparison of single-carrier and multi-carrier approach in terms of channel frequency selectivity :

Design parameters for outdoor channel	Required data rate	1 Mbps
	RMS delay spread, τ_{rms}	10 μs
	Channel coherence bandwidth, $B_c = \frac{1}{5\tau_{rms}}$	20 kHz
	Frequency selectivity condition	$\sigma > \frac{T_{sym}}{10}$
Single-carrier approach	Symbol duration, T_{sym}	1 μs
	Frequency selectivity	$10 \mu s > \frac{1 \mu s}{10} \implies \text{YES}$
	ISI occurs as the channel is frequency selective	
Multi-carrier approach	Total number of subcarriers	128
	Data rate per subcarrier	7.8125 kbps
	Symbol duration per subcarrier	$T_{carr} = 128 \mu s$
	Frequency selectivity	$10 \mu s > \frac{128 \mu s}{10} \implies \text{NO}$
	ISI is reduced as flat fading occurs. CP completely removes the remaining ISI; and also inter-block interference is removed	

The number of substreams is chosen to ensure that each subchannel has a bandwidth less than the coherence bandwidth of the channel, and therefore, the subcarriers experience relatively flat fading. Thus, the ISI on each subcarrier is small.

As seen from Fig.2.1 that the multicarrier modulation scheme with N subcarriers requires a bank of N local oscillators to modulate N data symbols. Therefore, when the number of subcarriers is large then it is difficult to accommodate a large number of local oscillators in the system. As seen from Fig. 2.2, we also require a bank of N correlators for demodulating the multicarrier signal. The above mentioned problems can be avoided by using OFDM as a MCM.

2.4 ORTHOGONALITY

Orthogonal frequency division multiplexing (OFDM) is a muticarrier modulation scheme, where the frequencies of the subcarriers are harmonically related. In other words, a multicarrier modulation scheme with orthogonal subcarriers is called as OFDM. Let $\{X_k\}_{k=0}^{N-1}$ be the set of complex symbols to be transmitted by multicarrier modulation, the continuous time domain MCM signal can be expressed as

$$\begin{aligned}
 x(t) &= \sum_{k=0}^{N-1} X_k \exp(j2\pi f_k t) & 0 \leq t \leq T_s \\
 &= \sum_{k=0}^{N-1} X_k \varphi_k(t) & 0 \leq t \leq T_s
 \end{aligned}$$

$$\varphi_k(t) = \begin{cases} \exp(j 2\pi f_k t) & 0 \leq t \leq T_s \\ 0 & \text{otherwise} \end{cases}$$

where $f_k = f_0 + k\Delta f$ and for $k = 0, 1, 2, \dots, N-1$. The subcarriers become orthogonal if modulation scheme is called OFDM, where T_s and Δf are called the OFDM symbol duration and the subcarrier frequency spacing respectively.

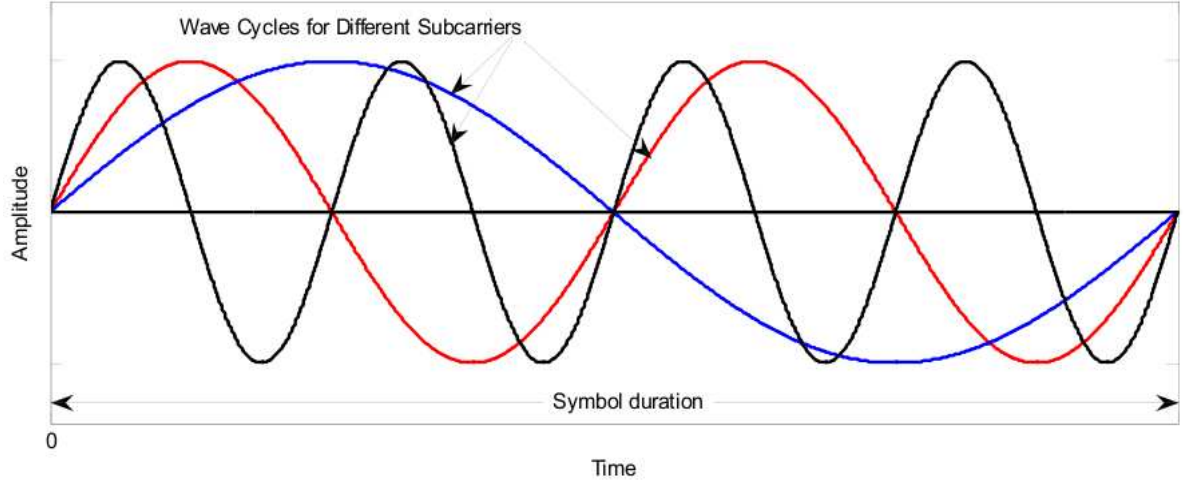


Figure 2.3: Time domain representation of the signal waveforms to show orthogonality among the subcarriers

In case of orthogonal subcarriers $x(t)$ denotes a time domain OFDM signal. The orthogonality among sub carriers can be viewed in time domain as shown in Fig. 2.3. Each curve represents the time domain view of the wave for a subcarrier. As seen from Fig. 2.3, in a single OFDM symbol duration, there are integer numbers of cycles of each of the subcarriers.

Because of the orthogonality condition, we have

$$\begin{aligned} & \frac{1}{T_s} \int_0^{T_s} \varphi_k(t) \varphi_l^*(t) dt \\ &= \frac{1}{T_s} \int_0^{T_s} e^{j 2\pi (f_k - f_l)t} dt \\ &= \delta[k - l] \\ \delta[n] &= \begin{cases} 1 & \text{if } n = 0 \\ 0 & \text{otherwise} \end{cases} \end{aligned}$$

Using above property, the OFDM signal can be demodulated as

$$\begin{aligned}
 &= \frac{1}{T_s} \int_0^{T_s} x(t) e^{j 2 \pi f_k t} dt \\
 &= \frac{1}{T_s} \int_0^{T_s} \left(\sum_{l=0}^{N-1} x_l(t) \varphi_k(t) \right) \varphi_l^*(t) dt \\
 &= \sum_{l=0}^{N-1} x_l \delta[k-l] \\
 &= x_k
 \end{aligned}$$

2.5 CYCLIC PREFIX

In ideal conditions the OFDM signal can be demodulated without any interference between the subcarriers. But in case of time dispersive channel, the orthogonality between the subcarriers gets disturbed because the demodulator correlation interval for one path will overlap with the symbol boundary of different path, it can be observed from Fig. 2.4. Thus, the integration interval will not necessarily correspond to an integer number of periods of complex exponentials of that path as the modulation symbols may differ between consecutive symbol intervals. As a consequence, there will not only be inter-symbol interference within a subcarrier but also interference between subcarriers.

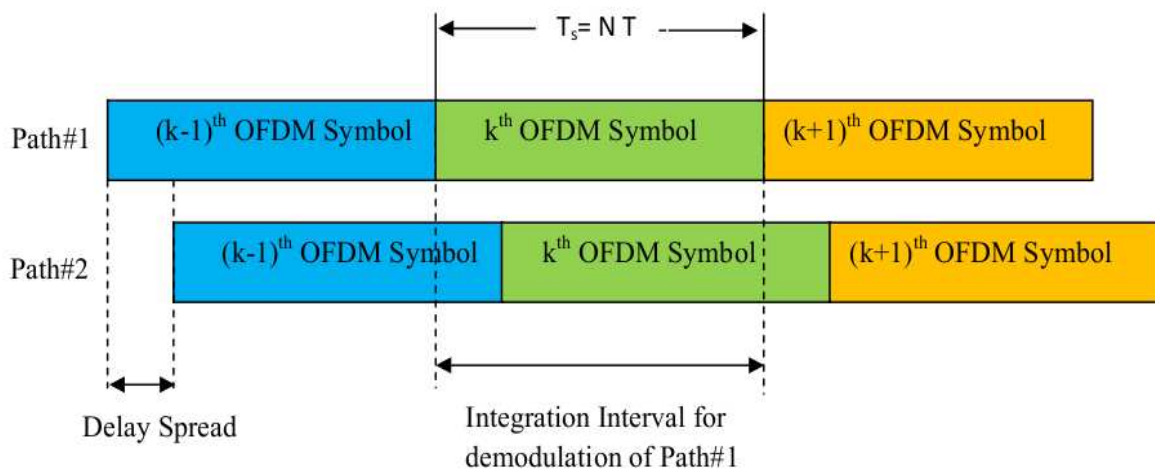


Figure 2.4: The time dispersion and corresponding received signals timing

To deal with this problem and to make an OFDM signal truly insensitive to time dispersion of the radio channel, cyclic-prefix (CP) insertion is typically used. As illustrated in Fig. 2.5, cyclic-prefix insertion implies that the last part of the OFDM symbol is copied and inserted at the beginning of the OFDM symbol. Cyclic-prefix insertion thus increases the length of the OFDM symbol duration from T_s to $T_s + T_{CP}$, where T_{CP} is the length of the cyclic prefix. As illustrated in Fig. 2.6, if the correlation at the receiver side is still carried out over a time interval T_s , subcarrier orthogonality will be preserved in case of a time-dispersive channel, as long as the span of the time dispersion is shorter than the length of cyclic-prefix. At the receiver side, the corresponding samples are discarded before OFDM subcarrier demodulation i.e. before DFT processing.

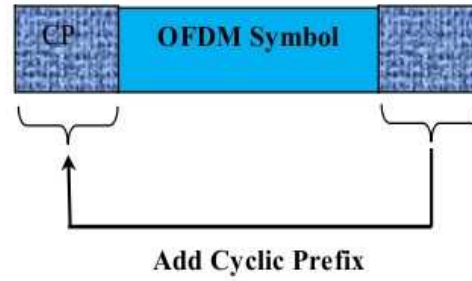


Figure 2.5: Cyclic Prefix

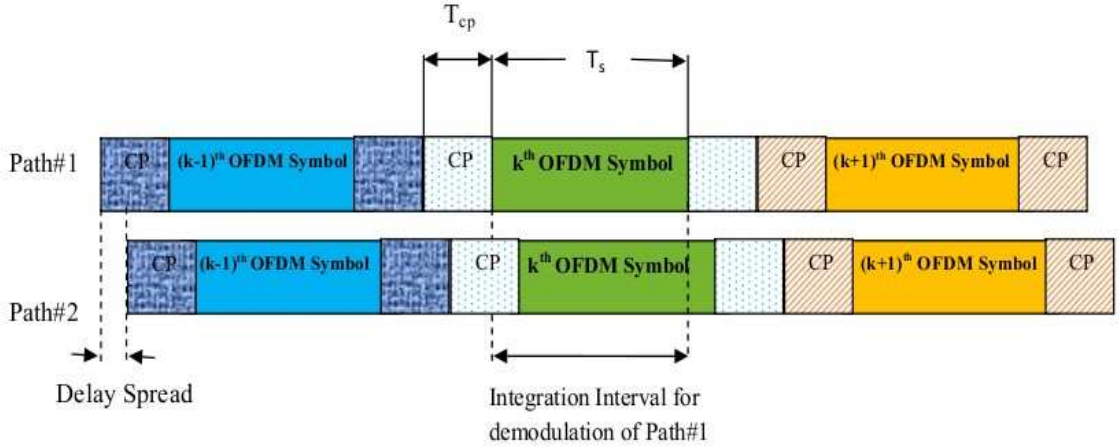


Figure 2.6: Time dispersion and corresponding received signal using cyclic prefix insertion

A cyclic-prefix insertion of N_{CP} samples is beneficial, when an OFDM symbol $x[n]$ is passed through dispersive channel ($h[n]$) with maximum delay spread of $N_{CP} + 1$ samples. Since CP values are repetition of the last (N_{CP}) sample values of the symbol, it is equivalent to conversion of the linear convolution of $x[n]$ and $h[n]$ into circular convolution. Because of the

circular convolution operation in time domain, the DFT of the received signal is a simple multiplication of the DFTs of $x[n]$ and $h[n]$, which makes it trivial to recover the transmitted symbol by a simple one tap equalizer.

Cyclic prefix insertion also avoids inter block interference, because by definition, when an input signal of length $N+N_{CP}$ is applied to a time dispersive channel of length $N_{CP}+1$, output of the channel produces $N+2N_{CP}$ samples. Out of $N+2N_{CP}$ samples, first N_{CP} samples may contain interference from preceding OFDM symbol, and therefore these are discarded, similarly the last N_{CP} samples may disperse into subsequent OFDM symbols and these are also discarded leaving exactly N samples. By using these N samples of the output signal, the N information data symbol can be easily recovered without IBI.

The drawback of cyclic-prefix insertion is that only a fraction $T_s/(T_s + T_{CP})$ of the received signal power is actually utilized by the OFDM demodulator, implying a corresponding power loss in the demodulation. In addition to this, cyclic-prefix insertion also implies a corresponding loss of bandwidth efficiency.

2.6 OFDM TRANSMITTER AND RECEIVER

A simplified block diagram of OFDM modulator is shown in Fig. 2.7. The input serial data stream is passed through a serial-to-parallel converter, which splits the input data stream into a number of parallel subchannels. The data in each of the subchannel is applied to a modulator, such that for N subchannels there are N modulators whose carrier frequencies are $f_0, f_1, \dots, f_k, \dots, f_{N-1}$. The carrier frequency spacing between two adjacent subchannel is Δf and the overall bandwidth of N modulated subchannels is $N\Delta f$. We may view the serial-to-parallel convertor as applying every N th symbol to a modulator. This has the effect of interleaving the symbols into each modulator, e.g. $X_0, X_N, \dots, X_{2N}, \dots, X_{kN}, \dots$ are applied to the subcarrier, whose carrier frequency is f_0 .

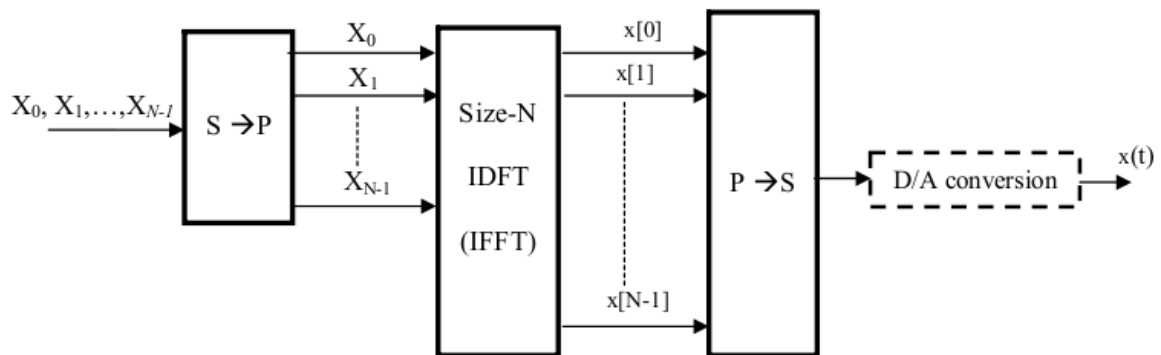


Figure 2.7: OFDM modulator

The sampled version of time domain baseband OFDM signal can be expressed as

$$x\left(\frac{nT_s}{N}\right) = \sum_{k=0}^{N-1} X_k \exp\left(\frac{j2\pi f_k nT_s}{N}\right) \quad 0 \leq n \leq N-1$$

Without loss of generality, setting $f_0 = 0$, then $f_k T_s = k$ and (2.6) becomes

$$x\left(\frac{nT_s}{N}\right) = \sum_{k=0}^{N-1} X_k \exp\left(\frac{j2\pi kn}{N}\right)$$

Therefore, the discrete time baseband OFDM signal of (2.7) can be expressed as

$$x\left(\frac{nT_s}{N}\right) = \sum_{k=0}^{N-1} X_k \exp\left(\frac{j2\pi kn}{N}\right)$$

where IDFT denotes the inverse discrete Fourier transform. Therefore, in OFDM system subcarrier modulation can be performed by using the IDFT block. The inverse fast Fourier transform (IFFT) algorithm provides an efficient way of implementing the IDFT operation. Therefore, when the number of subcarriers is large, then system's computational complexity may be reduced by using IFFT for performing the subcarrier modulation as shown in Fig. 2.7. In order to deal with the delay spread of wireless channels, a cyclic prefix is usually added at the transmitter to maintain the orthogonality between the subcarriers. Fig. 2.8 illustrates the basic principle of OFDM demodulation. The continuous time domain OFDM signal received at the receiver is first converted into digital and then applied to serial to parallel converter. After that FFT of the signal obtained from is performed to achieve the subcarrier demodulation. As seen from Fig. 2.8, that FFT operation used in OFDM demodulator eliminates the requirement of N correlators operating in parallel to demodulate the multicarrier modulator shown in Fig. 2.2.

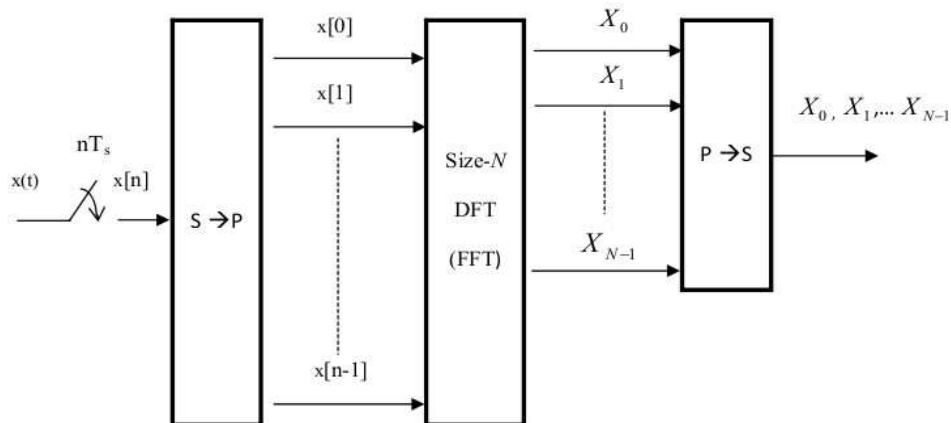
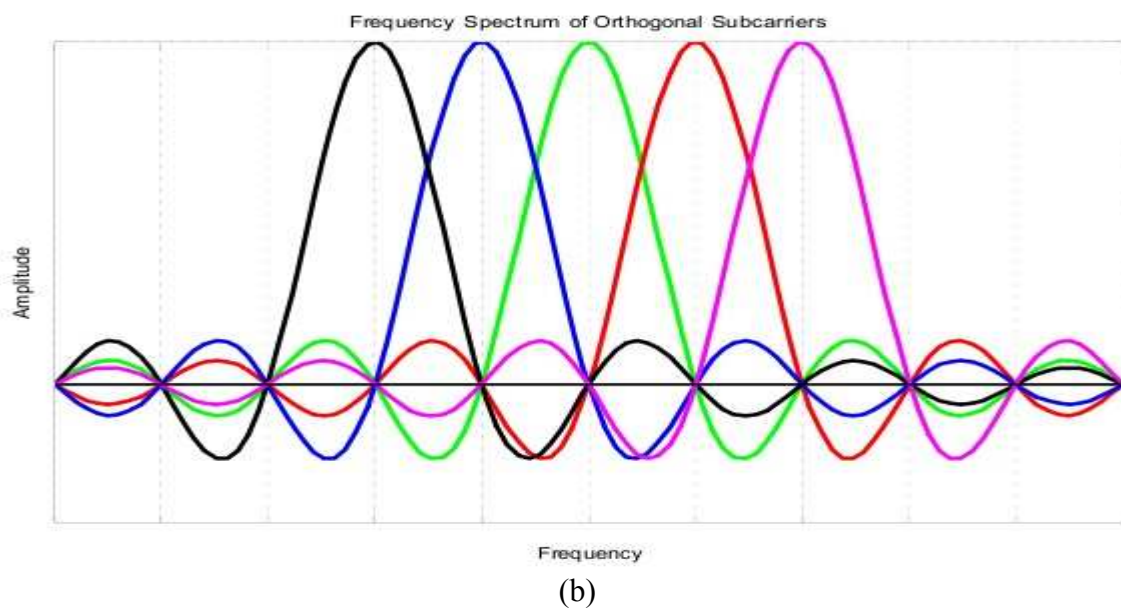
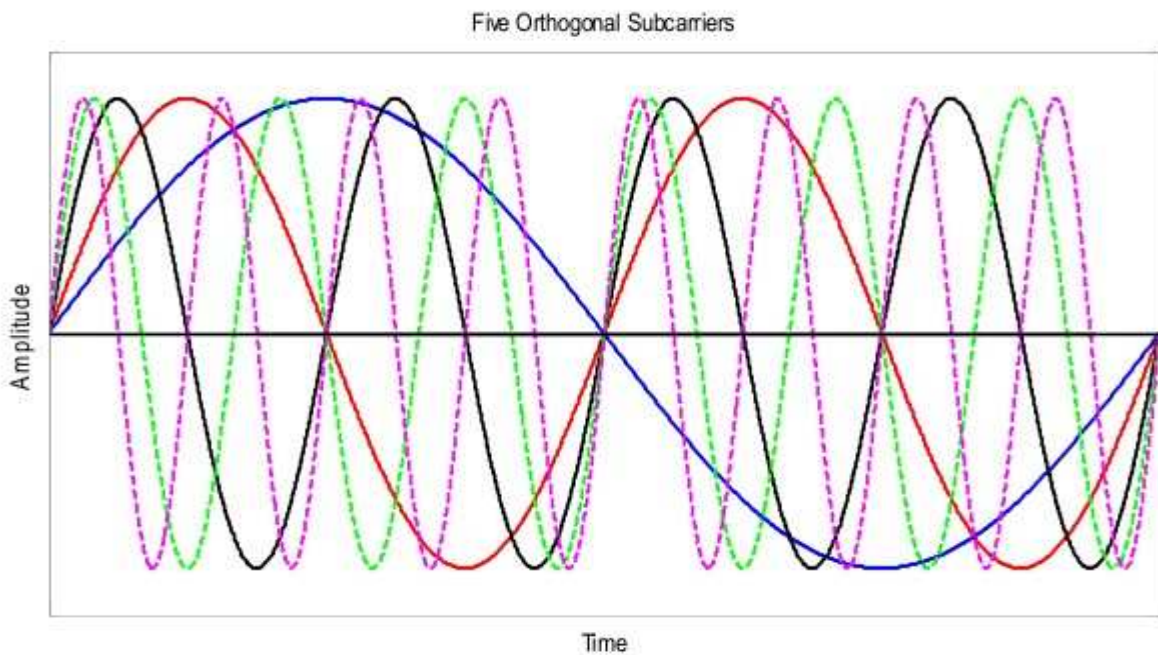


Figure 2.8: OFDM demodulator

Fig. 2.9(a) shows the waveforms of five orthogonal subcarriers used for modulation and corresponding frequency domain signal is shown in Fig. 2.9(b). Here, all of the subcarriers ensure orthogonality between them by having integer number of cycles per OFDM symbol duration. Fig. 2.9(c) shows the continuous time OFDM signal, when all of the subcarriers are modulated by binary data '1' and its frequency domain signal is shown in Fig. 2.9 (d).



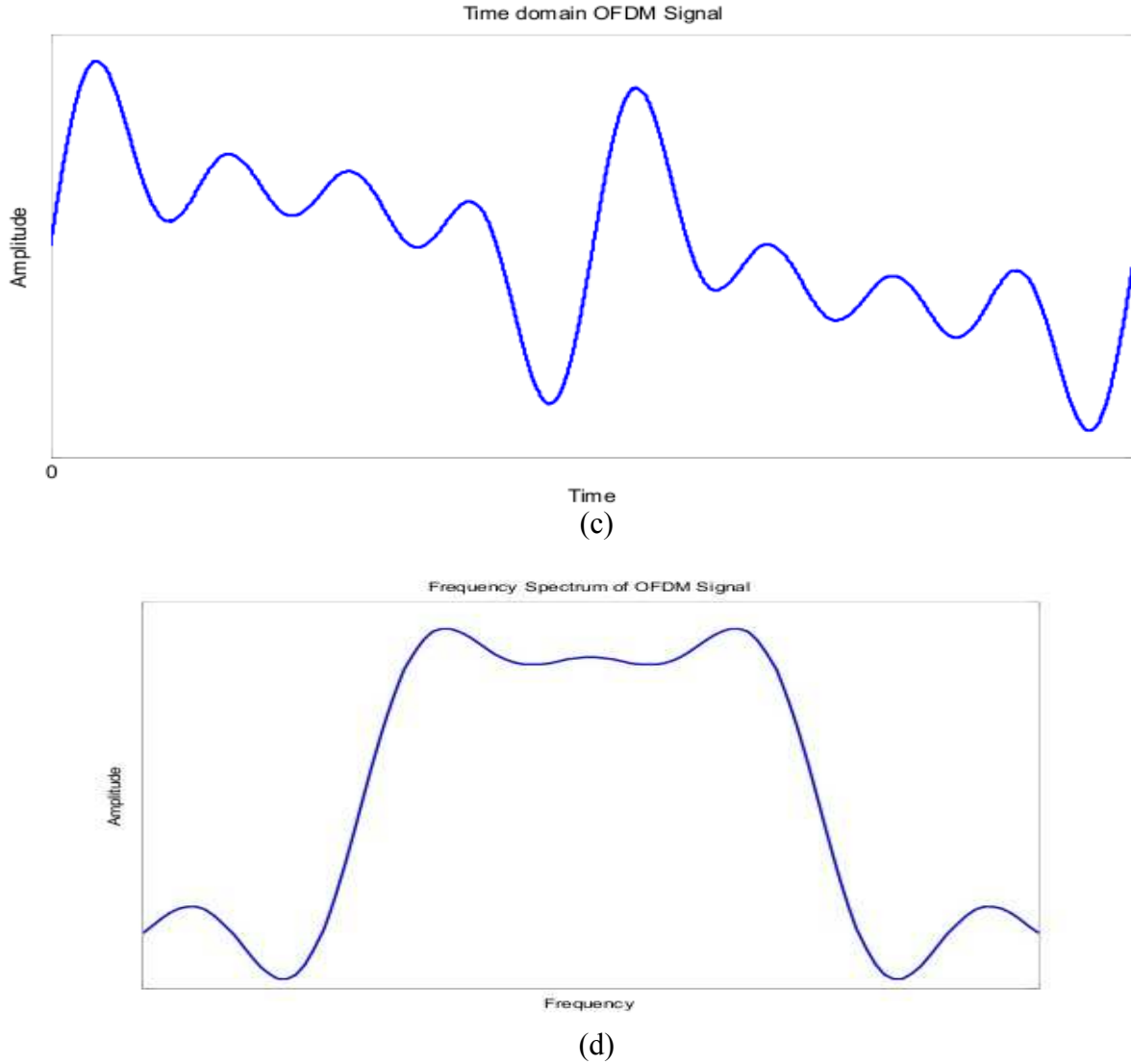


Figure 2.9: Construction of OFDM with 5 subcarriers (a) Time domain representation of all subcarriers (b) Frequency domain representation of subcarriers (c) Overall sum of subcarriers (Time domain) (d) Overall combined frequency response of subcarriers

A complete block diagram of an OFDM transceiver is shown in the Fig. 2.10. As seen from Fig. 2.10 the discrete time OFDM signal obtained from IFFT block is converted into serial OFDM symbol by using a serial to parallel converter and then a cyclic prefix of suitable length is inserted to combat the effect of ISI. Finally the discrete time OFDM signal is converted into analog OFDM signal and amplified to the desired power level. The obtained signal is transmitted over communication channel. The signal received $y(t)$ at the receiver has the effect of multipath propagation and AWGN($n(t)$). The received signal at the receiver is first converted into analog by using the D/A converter and cyclic prefix is removed. The obtained signal is applied to a serial to parallel converter and then subcarrier demodulation is performed by using

FFT operation. After that one tap frequency equalization can be utilized to cancel the effect of multipath fading channel and then passed through a parallel to serial converter to obtain serial data signal. Finally, signal is demodulated to get the desired data signal.

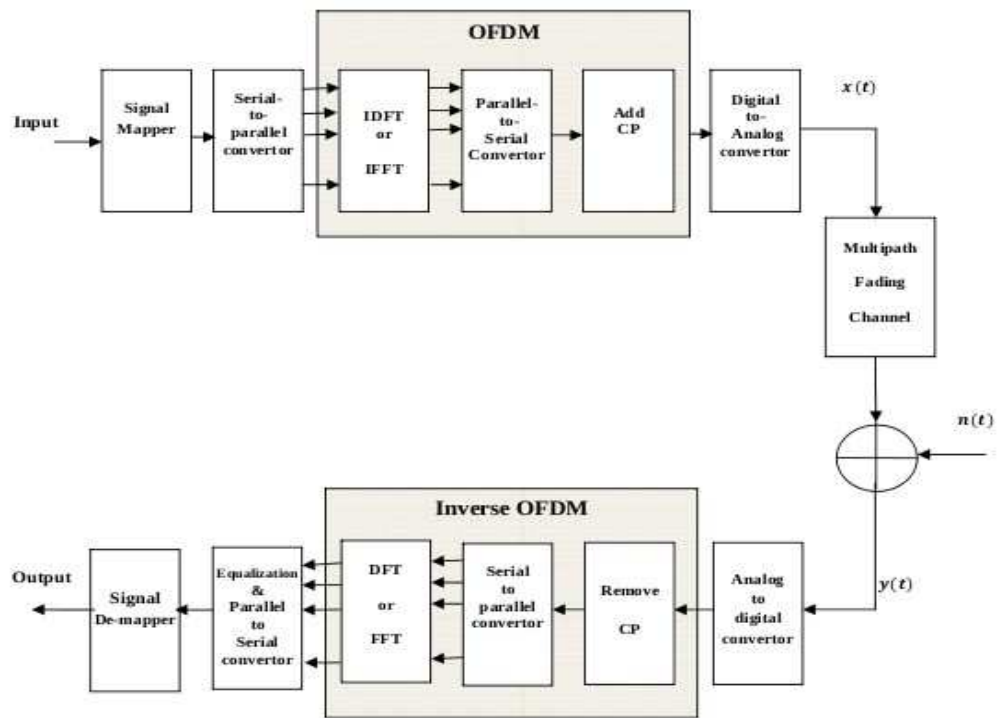


Figure 2.10: OFDM system

CHAPTER 3

PEAK TO AVERAGE POWER RATIO

Practical communication systems are usually peak power limited. An OFDM signal consists of a large number of independently modulated subcarriers, which on coherent addition may produce a high instantaneous peak with respect to the average signal level. High power amplifiers (HPA's) are used to amplify the time domain OFDM signal to the desired power level. In order to deal with the large fluctuations in the envelope of OFDM signal, HPA's are required to have a large linear range. Such HPA's are costly, bulky and difficult to design. If an HPA with limited linear range is utilized for amplification, it may operate near saturation and can cause out-of-band radiations and in-band distortion. The OOB distortion/noise is a major concern, especially in wireless communications, where large differences in signal strength from a mobile transmitter impose stringent requirements on adjacent channel interference (ACI). To accommodate large envelope fluctuations of the OFDM signal, the digital to analog converter (DAC) and analog to digital converter (ADC) are also required to have a wide dynamic range, which further increases the cost and complexity of the OFDM system. The recent interest in the application of OFDM to present and next generation wireless communication networks has triggered the development of numerous schemes to combat this problem.

In addition to this, OFDM system requires tight frequency synchronization in comparison to single carrier systems, because in OFDM, the subcarriers are narrowband. Therefore, it is sensitive to small frequency offset between the transmitted and the received signal, which may arise due to Doppler Effect in the channel, or due to mismatch between transmitter and receiver local oscillator frequencies. This carrier frequency offset (CFO) disturbs the orthogonality of the subcarriers and the signal on any particular subcarrier will not remain independent of the remaining subcarriers. This phenomenon, known as inter-carrier interference (ICI), is another challenge in the error-free demodulation and detection of OFDM symbols.

3.1 PEAK-TO-AVERAGE POWER RATIO

In general, the PAPR of a continuous time baseband OFDM signal $x(t)$ of (2.1) is defined as the ratio of the maximum instantaneous power to its average power

$$PAPR(x(t)) = \frac{\max_{0 \leq t \leq T_s} [|x(t)|^2]}{P_{av}}$$

where P_{av} is the average power and can be computed in frequency domain because IFFT is a unitary transformation.

3.1.1 PAPR OF BASEBAND OFDM SIGNAL

The discrete time baseband OFDM signal is defined in (2.9). The PAPR of the discrete time OFDM signal determines the complexity of the digital circuitry in terms of the number of bits necessary to achieve the desired signal to quantization noise ratio during signal digitization and recovery. To better approximate the PAPR of a continuous time OFDM signal, the discrete time OFDM signal is to be obtained by L times oversampling. The oversampled discrete time OFDM signal can be obtained by performing LN point IFFT on the data block with $(L-1)N$ zero padding as follows:

$$x[n] = \frac{1}{\sqrt{N}} \sum_{k=0}^{N-1} X_k \exp\left(\frac{j2\pi kn}{LN}\right), 0 \leq n \leq LN-1$$

The PAPR of the oversampled OFDM signal of (3.2) becomes

$$PAPR(x[n]) = \frac{\max_{0 \leq n \leq LN-1} [|x[n]|^2]}{E[|x[n]|^2]}$$

where $E[.]$ denotes the expectation operator.

3.1.2 PAPR OF BANDPASS OFDM SIGNAL

For large values of N , the power spectral density of band-limited OFDM signal has rectangular shape; therefore pulse shaping filter is usually not required. The bandpass OFDM signal can be expressed as

$$\begin{aligned} x_{BP}(t) &= \text{Re}\{x(t)e^{j2\pi f_c t}\} \\ &= \text{Re}\{x(t)\}\cos(2\pi f_c t) - \text{Im}\{x(t)\}\sin(2\pi f_c t) \end{aligned}$$

where f_c , $\text{Re}\{.\}$ and $\text{Im}\{.\}$ denotes the carrier frequency, the real and imaginary parts respectively. From (3.5), the peak value of RF signal is same as that of the baseband OFDM signal of (2.1) and the peak power becomes

$$\max\{|x_{BP}(t)|^2\} = \max\{|x(t)|^2\}$$

The average power of bandpass OFDM signal can be calculated as

$$\begin{aligned} E[|x_{BP}(t)|^2] &= E[|\operatorname{Re}\{x(t)e^{j2\pi f_c t}\}|^2] \\ &= E[|\operatorname{Re}\{x(t)\}\cos(2\pi f_c t) - \operatorname{Im}\{x(t)\}\sin(2\pi f_c t)|^2] \\ &= \frac{1}{2} E[|x(t)|^2] \end{aligned}$$

The PAPR of the bandpass OFDM signal can be calculated using (3.6) and (3.7) as follows

$$\begin{aligned} \text{PAPR}\{x_{BP}(t)\} &= \frac{\max_{0 \leq t \leq T_s} [|x_{BP}(t)|^2]}{E[|x_{BP}(t)|^2]} \\ &= 2 \left(\frac{\max_{0 \leq t \leq T_s} [|x(t)|^2]}{P_{av}} \right) \end{aligned}$$

$$\text{PAPR}\{x_{BP}(t)\} = 2 \text{PAPR}\{x(t)\}$$

Hence, we can say that the PAPR of bandpass OFDM signal is approximately twice the PAPR of baseband signal.

3.1.3 UPPER BOUND OF THE PAPR

The upper bound on PAPR can be calculated using the fact that the highest peak in OFDM signal results from the superposition of a large number of statistically independent subcarriers having the same initial phase. The average power level of discrete time OFDM signal can be calculated as

$$\begin{aligned} E[|x[n]|^2] &= E\left[\frac{1}{N} \sum_{k_1=0}^{N-1} \sum_{k_2=0}^{N-1} X(k_1)X^*(k_2)e^{j2\pi n(k_1-k_2)/N}\right] \\ &= \frac{1}{N} \sum_{k=0}^{N-1} E[|X(k)|^2] = \frac{N}{N} = 1 \end{aligned}$$

Similarly, the maximum power of the discrete time OFDM signal can be calculated as

$$\max\{|x(n)|^2\} = \max\left\{\frac{1}{N} \sum_{k=0}^{N-1} \sum_{k_2=0}^{N-1} X(k_1)X^*(k_2)e^{j2\pi n(k_1-k_2)/N}\right\}$$

For $k_1 = k_2$, the maximum power occurs when all the subcarriers are added with same initial phase

$$\max \left\{ |x[n]|^2 \right\} = \frac{1}{N} \sum_{k=0}^{N-1} \max \left\{ |X(k)|^2 \right\} = \frac{N^2}{N} = N$$

From above equations $\text{PAPR}\{x(t)\} = N$

Therefore, the worst case PAPR of a discrete time OFDM signal is directly proportional to the number of subcarriers. In some literature, crest factor (CF) is used in place of PAPR to characterize the envelope fluctuation of the OFDM signal. CF is defined as the maximum signal value divided by the RMS value of the signal. Therefore, CF is simply the square root of PAPR. In Fig. 3.1 a plot for CF of a time domain OFDM signal with 16 subcarriers having same initial phase is shown to verify the result obtained in (3.15). It can be seen from Fig. 3.1 that the maximum value of the CF for OFDM signal with 16 subcarriers is 4. Hence, worst case PAPR of OFDM signal with 16 subcarriers has a value 16.

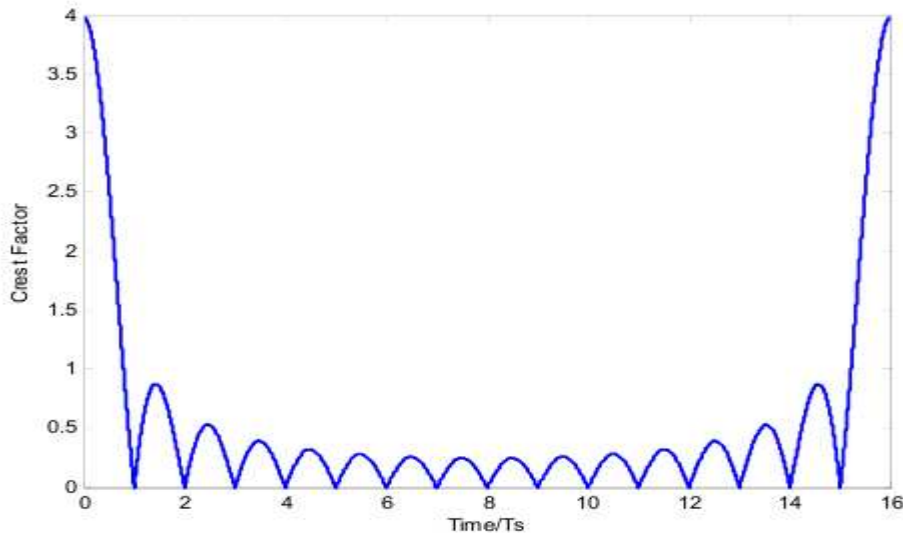


Figure 3.1: Square root of PAPR for an OFDM signal with 16 subcarrier having same initial phase

3.2 PDF OF OFDM SIGNAL

For the OFDM system shown in Fig. 2.10, if we assume that the input data stream is statistically independent and identically distributed (i.i.d) then the real and imaginary parts of $x[n]$ are uncorrelated and orthogonal. From central limit theorem, it follows that, for large values of N , the real and imaginary parts of $x[n]$ are independent and identically distributed (i.i.d.) Gaussian random variables, each with zero mean and variance $\sigma^2 = E[|x[n]|^2]/2$. The

$$\Pr\{x[n]\} = \frac{1}{\sqrt{2\pi\sigma^2}} \exp\left(-\frac{x^2[n]}{2\sigma^2}\right)$$

probability distribution of complex OFDM signals with large N is a complex Gaussian distribution given by following relation where $\Pr\{\cdot\}$ denotes the probability distribution function. where, σ^2 is the variance of $x[n]$.

$$\Pr\{|x[n]|\} = \frac{2|x[n]|}{\sigma^2} \exp\left(-\frac{|x[n]|^2}{\sigma^2}\right)$$

3.3 COMPLEMENTARY CUMULATIVE DISTRIBUTION FUNCTION OF PAPR

The complementary cumulative distribution (CCDF) is a parameter to characterize the peak power statistics of a digitally modulated OFDM signal. The CCDF of PAPR provides the information about the percentage of OFDM signals that have PAPR above a particular level. The magnitude of OFDM signal has Rayleigh distribution, while its power has chi-square distribution. The cumulative distribution function (CDF) of PAPR of an OFDM signal with N subcarriers is

$$\begin{aligned} \text{CDF}(\gamma_0) &= \Pr(\text{PAPR}(x[n]) \leq \gamma_0) \\ &= (1 - \exp(-\gamma_0))^N \end{aligned}$$

where γ_0 is the given threshold value of PAPR. Therefore, the complementary cumulative distribution function (CCDF) of PAPR becomes

$$\begin{aligned} \text{CCDF}(\gamma_0) &= \Pr(\text{PAPR}(x[n]) > \gamma_0) \\ &= 1 - (1 - \exp(-\gamma_0))^N \end{aligned}$$

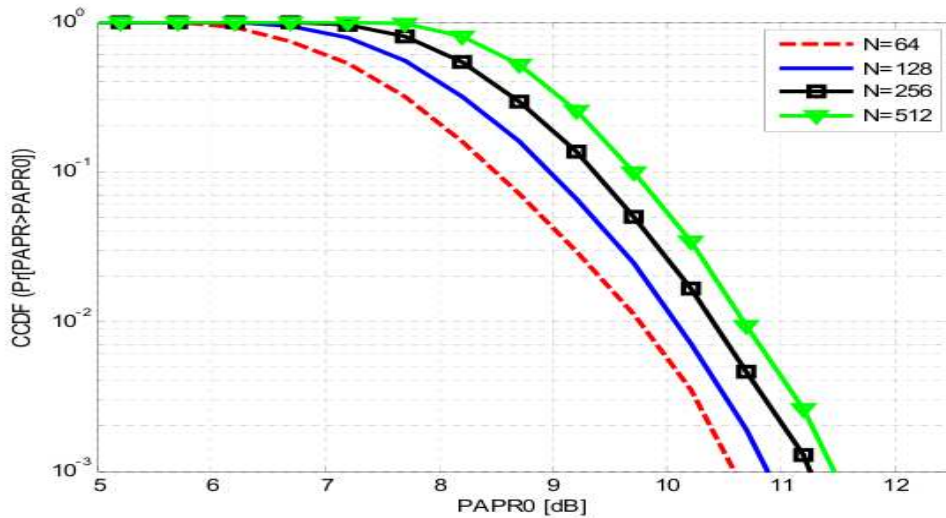


Figure 3.2: CCDF of PAPR for N=64,128,256,512

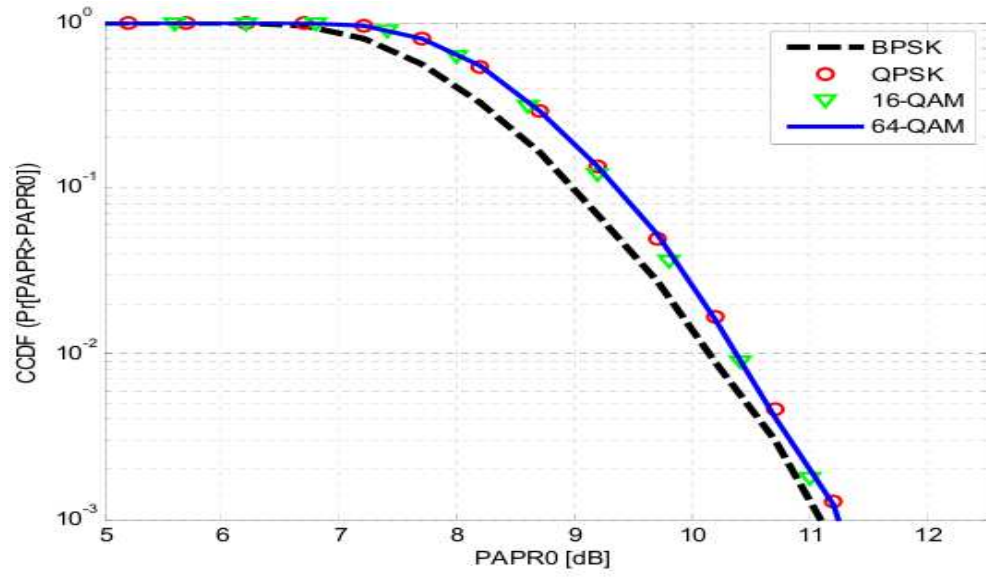


Figure 3.3: CCDF of PAPR for different modulation techniques

It has been found that PAPR performances of all modulation schemes under consideration are very close, except BPSK, which is observed to be slightly better than others.

CHAPTER 4

PAPR REDUCTION TECHNIQUES

Criteria For PAPR Reduction Method Selection:

The criteria of the PAPR reduction is to find the approach that it can reduce PAPR largely and at the same time it can keep the good performance in terms of the following factors as possible. The following criteria should be considered in using the techniques:

- i) The high capability of PAPR reduction is primary factor to be considered in selecting the PAPR reduction technique with as few harmful side effects such as in-band distortion and out-of-band radiation.
- ii) Low average power: Although it also can reduce PAPR through average power of the original signals increase, it requires a larger linear operation region in HPA(High Power Amplifier) and thus resulting in the degradation of BER performance.
- iii) Low implementation complexity: Generally, complexity techniques exhibit better ability of PAPR reduction. However, in practice, both time and hardware requirement for the PAPR reduction should be minimal.
- iv) No Bandwidth expansion: The bandwidth expansion directly results in the data code rate loss due to side information. Moreover, when the side information are received in error unless some ways of protection such as channel coding employed. Therefore, when channel coding is used, the loss in data rate is increased further due to side information. Therefore, the loss in bandwidth due to side information should be avoided or at least be kept minimal.
- v) No BER performance degradation: The aim of PAPR reduction is to obtain better system performance including BER than that of the original OFDM system. Therefore, all the methods, which have an increase in BER at the receiver, should be paid more attention in practice.
- vi) Without additional power needed: The design of a wireless system should always be take into consideration the efficiency of power.

The PAPR reduction schemes are majorly divided into two categories.

- a) Distortion Techniques
- b) Non-distortion Techniques

4.1 DISTORTION BASED TECHNIQUES

The schemes that introduce spectral re-growth belong to this category. Distortion based techniques are the most straightforward PAPR reduction methods. Furthermore, these techniques distort the spectrum, this spectrum distortion or “spectral re-growth” can be corrected to a certain extent by using filtering operation.

4.1.1 CLIPPING

Clipping is one of the simplest techniques to reduce the PAPR of OFDM signal. It reduces the peak of the OFDM signal by clipping the signal to the desired level. This operation can be implemented on discrete time samples prior to the DAC or by designing the power amplifiers with saturation level lesser than the OFDM signal dynamic range. The amplitude clipper limits the peak of the envelope of the input OFDM signal to a predetermined threshold value (γ_o) or otherwise passes the input signal unperturbed. The clipping operation can be mathematically defined as

$$x^c(t) = \begin{cases} x(t) & |x(t)| \leq \gamma_o \\ \gamma_o e^{j\angle x(t)} & |x(t)| > \gamma_o \end{cases}$$

where $x^c(t)$ and $\angle x(t)$ are the clipped OFDM signal and the phase of $x(t)$. It is a nonlinear operation and therefore causes both in-band distortion and out-of-band radiation. The in-band distortion is treated as noise and therefore results in error performance degradation. If clipping level γ_o is too small, then out-of-band radiation becomes more significant. The out-of-band radiation can be eliminated by using filtering operation but filtering operation causes peak re-growth in OFDM signal, and as a result the amplitude of time domain OFDM signal again exceeds the clipping level (γ_o). The BW efficiency of the OFDM system decreases due to spectral re-growth. The computational complexity of the clipping scheme is found to be the least in comparison to other distortion PAPR reduction schemes but at the same time its BER performance is very poor.

Iterative Clipping and Filtering

Jean Armstrong proposed the repeated clipping and filtering scheme, in which clipping and frequency domain filtering operations are repeated several times to reduce both the out-of-band radiation and PAPR to the desired level. The PAPR performance and amount of out-of-band radiation mainly depends on the number of iterations to be performed, more the number of iterations lesser is the value of out-of-band radiations and PAPR. But, the computational complexity of iterative clipping and filtering scheme increases with the number of iterations.

4.1.2 COMPANDING

Companding is another popular PAPR reduction scheme. Companding is a composite word formed by combining compressing and expanding. In this scheme, at the transmitter a signal with high dynamic range is applied to a compander and at the receiver a decompressing function (the inverse of companding function) is used to recover the original signal. Initially, it was used in digital communication systems to increase the dynamic range of digital to analog converters (DACs). The μ -law and A-law are the two most popular compressing functions used worldwide. Wang et al. proposed a scheme a μ -law companding scheme to reduce the PAPR of OFDM signal. According to this scheme, the time domain OFDM signal ($x[n]$) is applied to a μ -law compressor to produce a companded OFDM signal given by

$$x_{\mu c}[n] = \frac{A \operatorname{sgn}(x[n]) \ln \left[1 + \left| \frac{x[n]}{A} \right| \right]}{\ln(1 + \mu)}$$

where, A is the peak value of the OFDM signal before companding and μ is the parameter controlling nonlinearity of the companding function. $\operatorname{sgn}(\cdot)$ and $\ln(\cdot)$ are the standard signum and natural logarithmic function respectively. The discrete time domain companded OFDM signal is converted to analog signal using D/A converter and then amplified using HPA to achieve the desired power level. The amplified signal is then transmitted over the communication channel. At the receiving end, the received signal ($r[n]$) is applied to the expander to recover the transmitted time domain signal. The time domain OFDM signal at expander output is given by

$$x_{\mu e}[n] = \frac{A \exp \left\{ \frac{r[n]}{A \operatorname{sgn}(r[n])} \ln(1 + \mu) \right\}}{\mu \operatorname{sgn}(r[n])}$$

Here, the received signal ($r[n]$) is nothing but the companded OFDM signal ($x_{\mu c}[n]$) corrupted by quantization and channel noise. The real and the imaginary parts of the complex

time domain OFDM signal have Gaussian distribution. But, after applying the μ -law companding scheme, the PDF of real and imaginary parts no longer remains Gaussian distributed. 4.1 shows the probability distribution function of real part before and after companding of OFDM signal.

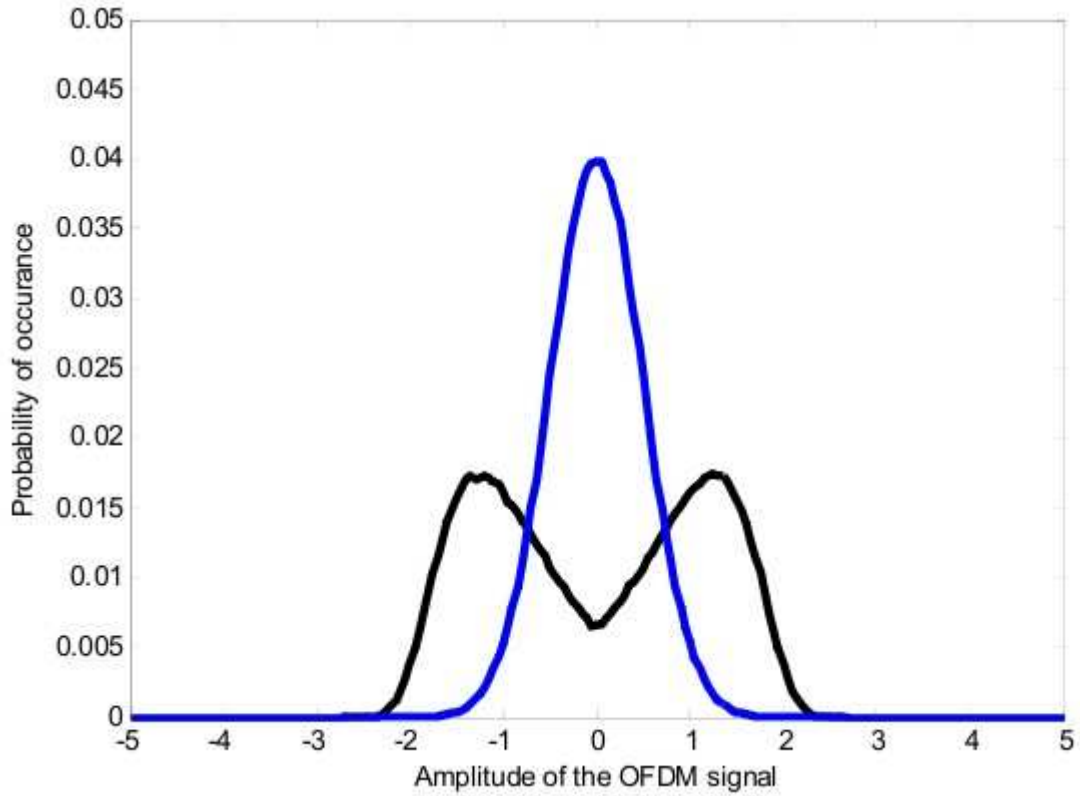


Figure 4.1: PDF of real part of original and μ -law companded OFDM signal amplitude

It can be easily observed from the Fig. 4.1 that due to μ -law companding operation the probability of real part of the OFDM signal with small amplitude gets decreased whereas the probability of OFDM signal with large amplitude gets increased. A similar phenomenon can be observed for the imaginary part of the OFDM signal. Therefore, the average power of the OFDM signal increases. In μ -law companding scheme the peak value of the OFDM signal before and after companding remain same, which keeps peak power of the OFDM signal unchanged. Therefore, μ -law companding scheme decreases the PAPR of the OFDM signal. By controlling the parameter μ , the average power of the OFDM signal can be controlled and hence the desired value of PAPR can be obtained. The overall PAPR reduction capability and BER performances of μ -law companding scheme is found to be better than clipping and filtering scheme.

Due to increase in the average power level of the OFDM signal, the overall error performance of the system degrades in comparison to OFDM signal without companding; higher the value of the μ , better is the PAPR reduction, but at the same time, error performance degradation is also higher. Fig. 4.2 shows the CCDF of PAPR for normal and μ -law companded OFDM signal. In this simulation, we have considered a QPSK modulated OFDM system with $N=256$ subcarriers.

We have used $\mu=\sqrt{254}$ for companding the OFDM signal. It can be observed from Fig 4.2 that μ -law companding scheme, achieves a PAPR reduction capability of 5.2dB for a CCDF of 10^{-4} .

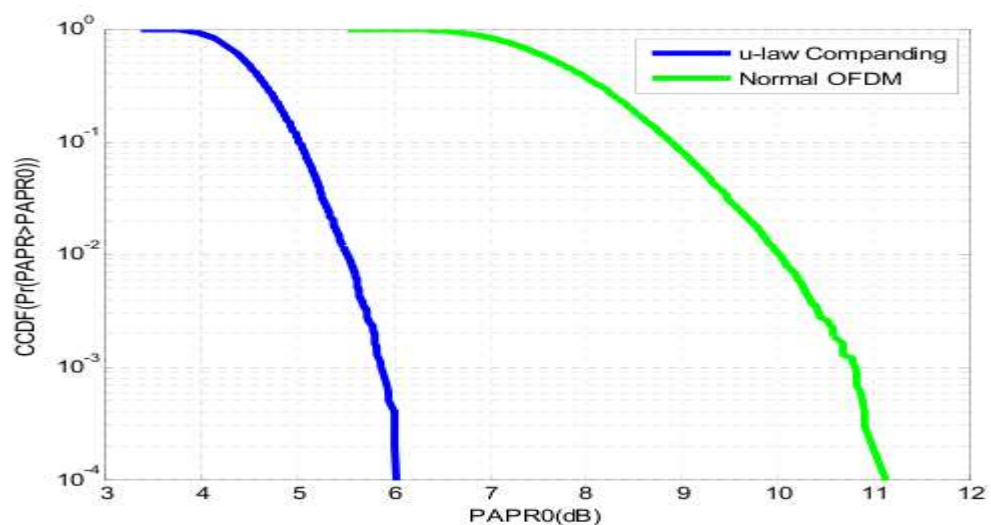


Figure 4.2: Comparison of PAPR performance of normal and μ -law companded OFDM signal

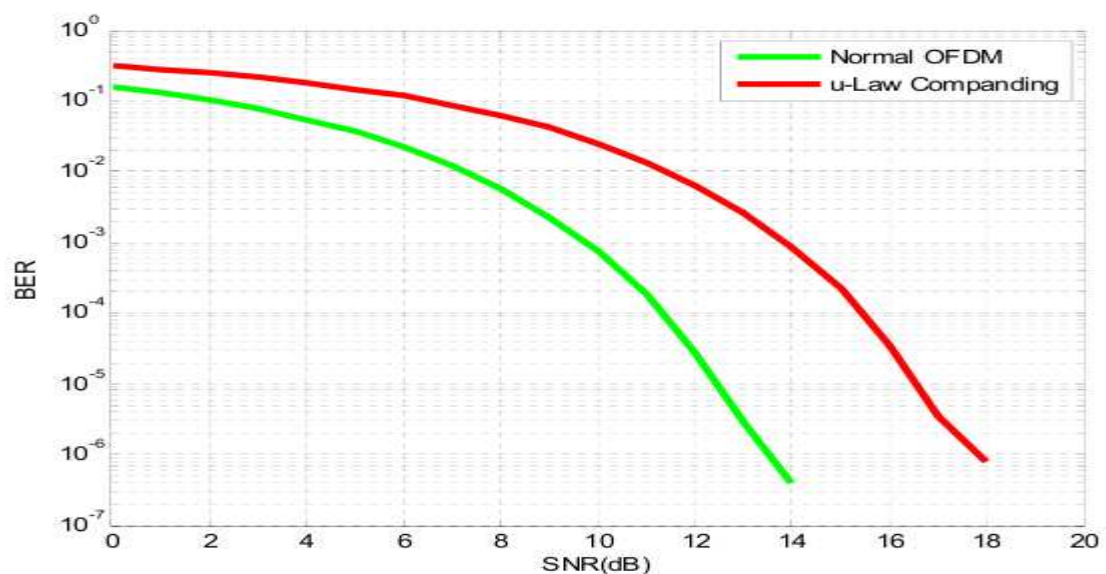


Figure 4.3 BER performance comparison of Normal OFDM and μ -law companding

The BER performance of the normal and μ -law companded OFDM signal is shown in Fig. 4.3. The BER performance of OFDM system utilizing μ -law companding is worse than the normal OFDM signal. Normal OFDM system requires 4dB less SNR to achieve a BER of 10^{-5} .

All of the techniques discussed in this section do not require any side information to recover the data signal at the receiver and hence the data rate of the system remains same even after applying PAPR reduction scheme. The computational complexity of these schemes is also very less. However, the price paid for using a distortion technique is in-band distortion, out-of-band radiation and ICI, which adversely affects the bit error rate (BER) of the system.

4.2 NON-DISTORTION TECHNIQUES

These types of PAPR reduction schemes do not distort the shape of the OFDM signal and therefore no spectral re-growth take place.

4.2.1 SELECTED MAPPING

SLM is another popular distortion-less PAPR reduction technique first described by Cimini et al. In this scheme, a set of U independent data sequences is generated by multiplication of a

block of N modulated data symbols $\{X_k\}_{k=0}^{N-1}$ with a phase sequence set containing U phase vectors of length N . The set of U independent signals can be mathematically expressed as follows

$$X_k^u = X_k \cdot P_k^u, \quad 1 \leq u \leq U \text{ \& } 0 \leq k \leq N-1$$

Here, each phase vector $\{P_k^u\}_{k=0}^{N-1}$ has a length N and its elements, i.e. Phase factors,

$$P_k^u \in \left\{ \phi_l = \exp\left(\frac{j2\pi l}{W}\right) \mid 0 \leq l \leq W-1 \right\}$$

where W denotes the number of phase factors. The set of U independent discrete-time OFDM signals x^u , $1 \leq u \leq U$ can be obtained from a set of U data sequences as

$$x^u[n] = \frac{1}{\sqrt{N}} \sum_{k=0}^{N-1} X_k^u \exp\left(\frac{j2\pi kn}{N}\right), \quad 0 \leq n \leq N-1$$

Out of these U signals, one of them satisfying following criterion is selected for transmission

$$x^o = \arg \min_{1 \leq u \leq U} \text{PAPR}(x^u)$$

where u , $1 \leq u \leq U$ is the index of phase vector in the phase sequence set that generates an OFDM signal with least PAPR. Therefore, the information about u should be transmitted along with each OFDM symbol, which requires $\log_2(U)$ bits, if straight binary coding is used to encode the SI. The SI bits are extremely important for data recovery at the receiver; therefore sometimes we sacrifice the data rate and allocate few redundant bits to ensure accurate recovery of u . But it further increases the loss in data rate of a SLM-OFDM system.

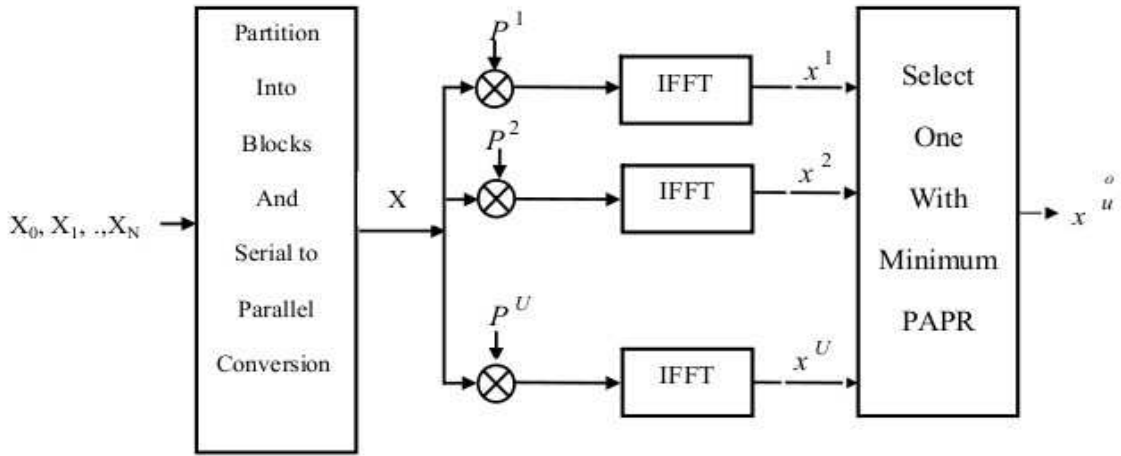


Figure 4.4: Block diagram of conventional SLM-OFDM transmitter

Fig. 4.5 shows comparison of the PAPR performance of SLMsystem for various values of U .

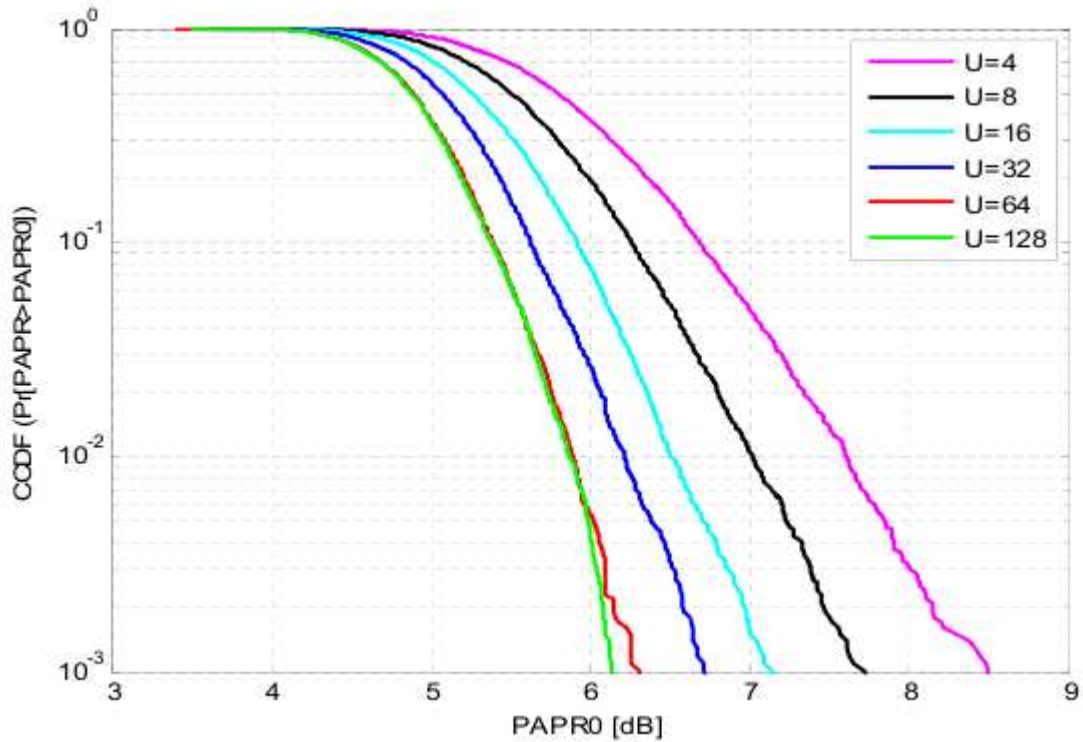


Figure 4.5: PAPR performance comparison of SLM-OFDM system for various values of U

In this simulation, we have considered a QPSK modulated OFDM signal with $N=64$ subcarriers. It can be seen from Fig. 4.5 that the PAPR reduction capability of SLM-OFDM system increases by increasing the value of the number of phase sequences (U) in phase sequence set. But, this gain in PAPR reduction capability is obtained at the cost of increased computational complexity because for a phase sequence set with U phase sequences requires U IFFT operations to find the OFDM signal with lowest possible PAPR (x^u). Moreover, higher the value of U , more is the number of bits required to encode the side information and therefore data rate loss is also more.

4.2.2 PARTIAL TRANSMIT SEQUENCES

PTS is one of the most popular distortion-less PAPR reduction scheme. In this scheme a block of N modulated data symbols $\{X_k\}_{k=0}^{N-1}$ is partitioned into S disjoint sub-blocks where $S < N$. After partitioning, S data sub-blocks are represented by $[X_k^s, s = 0, 1, 2, \dots, S-1, k = 0, 1, \dots, N-1]$, here the length of each data sub-block is N and all of them are disjoint in a sense that the value of X_k^s is non-zero only for one particular value of s , $s \in 0, 1, 2, \dots, S-1$, therefore we have

$$\{X_k\}_{k=0}^{N-1} = \sum_{s=0}^{S-1} X_k^s \quad k = 0, 1, \dots, N-1$$

After this, IFFT of each of the data sub-block is taken to obtain S partial transmit sequences x_s , given by

$$x_s(n) = \frac{1}{\sqrt{N}} \sum_{k=0}^{N-1} X_k^s e^{j \frac{2\pi kn}{N}} \quad s = 0, 1, 2, \dots, S-1; n = 0, 1, 2, \dots, N-1$$

The partial transmit sequences are multiplied by phase rotation factors $b(s)$ and all of them are combined to obtain a time domain OFDM signal (x') given by following expression

$$x' = \sum_{s=0}^{S-1} b(s) x_s$$

where $b(s)$ is the phase rotation factor for s^{th} data sub-block. Here, the objective of combining the partial transmit sequences after multiplication with phase factor is to obtain a time domain OFDM signal with lowest possible PAPR. Therefore, to find the optimal values of phase factors to achieve lowest possible PAPR of OFDM signal x' , following optimization criterion is used.

$$[b(0) \ b(1) \ \dots \ b(S-1)] = \arg \min_{[b(0) \ b(1) \ \dots \ b(S-1)]} \left\{ \max_{0 \leq n \leq N-1} |x'| \right\}$$

where $[b(0) b(1) \dots b(S-1)]$ are the optimized phase rotation factors for sub-blocks $X_k^0, X_k^1, \dots, X_k^{S-1}$, respectively. The block diagram of the PTS transmitter is shown in Fig. 4.6. The partitioning schemes for PTS based PAPR reduction schemes are majorly classified into (i) adjacent (ii) interleaved (iii) pseudorandom partitioning. It has been reported that PAPR reduction capability of PTS-OFDM system using pseudorandom partitioning is better than that of adjacent and interleaved partitioning schemes.

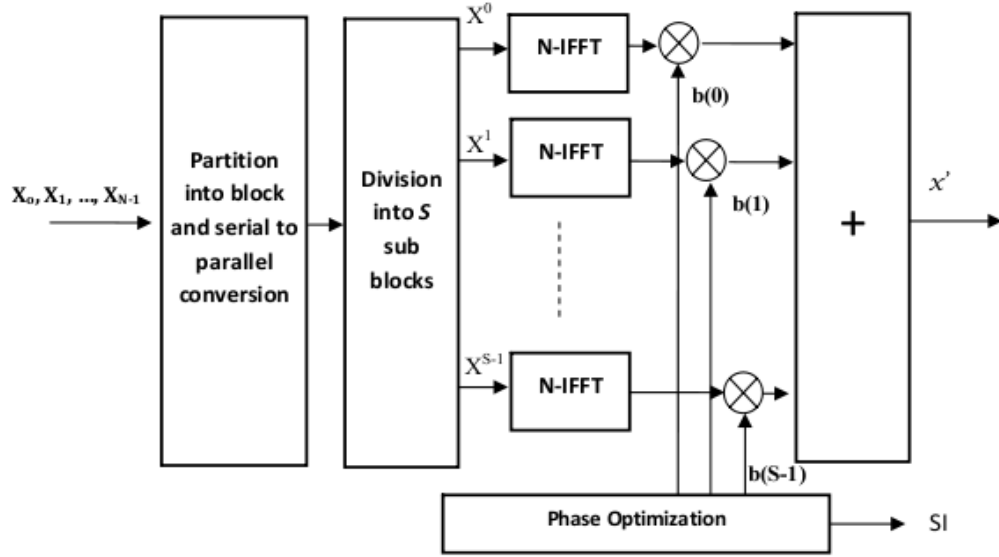


Figure 4.6: Block diagram of conventional PTS-OFDM system transmitter

The PAPR reduction capability of PTS-OFDM system increases by increasing number of partitions (S). But, in this scheme for S data sub-blocks, S IFFT operations are required to calculate x' , which results in high computational complexity. Therefore, the number of partitions (S) is restricted to 4.

The IFFT of x_s has to be multiplied with phase factor $b(s)$, if phase rotation factors have non-zero real and imaginary parts then it requires SN additional complex multiplications, which will further increase the computation complexity of the PTS scheme. In order to reduce the computational complexity incurred in the computation of x' , phase factor $b(s)$ should be pure rotational, and therefore chosen from the set $B = \{1, j, -1, -j\}$, here $b(s) \in B$. The optimum search algorithm, requires W^{S-1} iterations (searches) to find phase rotation factors, where W is the number of phase factors in phase set B. Many sub-optimal search algorithms have been proposed for finding $[b(0) b(1) \dots b(S-1)]$.

The information about the phase rotation factors $[b(0) b(1) \dots b(S-1)]$ used at the transmitter for PAPR reduction is required to be sent along with each OFDM symbol for data recovery at the receiver. The information used for this purpose is called side information (SI),

which reduces the effective data rate of PTS-OFDM system. If straight binary coding scheme is used then $\log_2 (W^{S-1})$ bits per OFDM symbol are required to encode the SI. The loss in data rate will further increase if any error control coding with low code rate is used for encoding the SI. Fig. 4.7 shows the PAPR performances of OFDM signal without PAPR reduction, PTS-OFDM system with 4 partitions and two phase factors (1,-1), and PTS-OFDM system with 4 partitions and four phase factors (1, j,-1, -j). In this simulation we have considered a QPSK modulated OFDM system with $N=256$ subcarriers.

The PAPR reduction capability of the PTS increases with the increase in the value of W . PTS with $W=2$ and $W=4$, achieve a PAPR reduction capabilities of 2.5dB and 3.5 dB respectively, for a CCDF of 10^{-3} , over OFDM signal without PAPR reduction.

The PAPR reduction capability of the PTS increases with the increase in the value of W . PTS with $W=2$ and $W=4$, achieve a PAPR reduction capabilities of 2.5dB and 3.5 dB respectively, for a CCDF of 10^{-3} , over OFDM signal without PAPR reduction. The PAPR reduction capability of PTS-OFDM system with $W=4$ is more than that of PTS-OFDM system with $W=2$ because for $M=W=4$ there are 64 alternative signals, whereas for $M=4$ and $W=2$ there are only 8 alternative signals. More is the number of alternative signals more is the PAPR reduction.

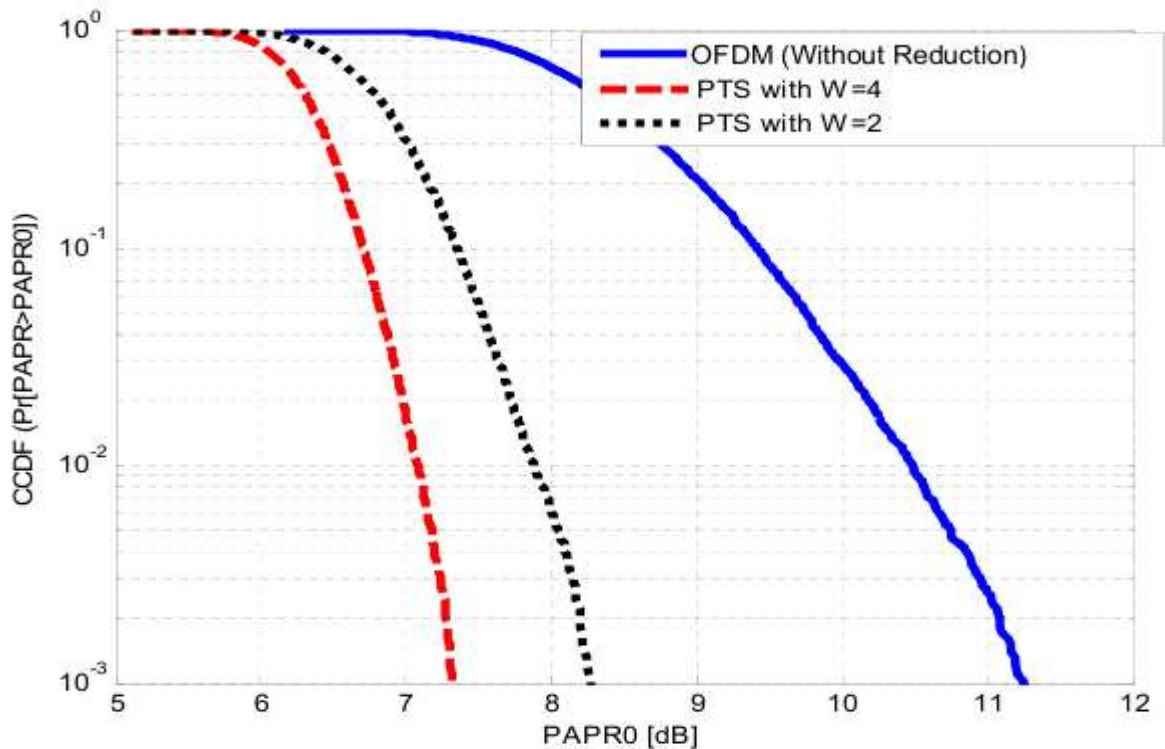


Figure 4.7 Comparison of PAPR performance of PTS-OFDM with $W=2$ and 4

4.2.3 TONE RESERVATION

Tone reservation was first described by Tellado and Cioffi in 1997. The basic idea is to reserve certain numbers (R) of subcarriers or tones for reducing the PAPR of the OFDM signal. The subcarriers or tones reserved for PAPR reduction are known as PAPR reduction tones (PRT). Here, the main objective is to choose the value of data signals to be transmitted on reserved tones to minimize the PAPR of time domain OFDM signal. The PAPR reduction capability of this scheme mainly depends on the number of PRTs and their location in the frequency band. The PRT locations are known in advance to both transmitter and receiver. The PRTs are not used for data transmission and therefore it results in data rate loss. Let $X = \{X_k\}_{k=0}^{N-1}$ and $Z = \{Z_k\}_{k=0}^{N-1}$ be the data and PRT blocks, the PRT locations in Z and locations of subcarriers for data transmission in X are chosen disjointly, such that their point wise multiplication $\{X_k \cdot Z_k\}_{k=0}^{N-1} = 0$ is zero. Consider a tone reservation scheme with R PRTs located at $i_0, i_1, \dots, i_r, \dots, i_{R-1}$, and the data symbols are transmitted only on the subcarriers with index k, $0 \leq k \leq N-1$ and $k \neq i_r, 0 \leq r \leq R-1$. After applying tone reservation scheme, the frequency domain OFDM signal (X^{TR}) is given by following expression

$$X^{TR} = \sum_{k=0}^{N-1} (X_k + Z_k)$$

The corresponding time domain OFDM signal $x^{TR}[n]$, $0 \leq n \leq N-1$ can be found as

$$x^{TR}[n] = \text{IFFT}(X^{TR}) = \text{IFFT}(X) + \text{IFFT}(Z)$$

$$x^{TR}[n] = x[n] + z[n], \quad 0 \leq n \leq N-1$$

where $x[n]$ and $z[n]$ are the N point IFFTs of X and Z respectively. In order to reduce the PAPR of the time domain OFDM signal, the peak is minimized by finding the optimal value of PRTs i.e. Z^{opt} . For this, one can utilize convex optimization technique, that can be cast as linear programming problem. To find Z^{opt} , projection on to convex set (POCS) or gradient search algorithm can be used.

In order to reduce data rate loss in TR scheme, tone injection (TI) scheme is proposed. In this scheme, the PRTs and data symbols can be transmitted on the same subcarriers. The basic idea of TI is to extend the constellation, such that one constellation point may correspond to more than one point in the extended constellation. In this scheme PRTs and data symbols are not mutually exclusive, therefore at the receiver; some efficient scheme to separate the PRTs has to be utilized. One of the solutions to this problem is to use PRTs of the type $Z_k = q \cdot a_k + q \cdot b_k$, where q is a positive integer, a_k and b_k are chosen for reducing the PAPR of OFDM signal. If we

choose $a_k = [-1, 0, 1]$ and $b_k = [-1, 0, 1]$ then for $q > 1$, each of the M-PSK or M-QAM modulated symbol corresponds to 9 different symbols of extended constellation, and therefore result in a constellation with $9M$ points. The expanded constellation symbol is given by

$$X_k^E = X_k + q.a_k + q.b_k$$

The average power of the signal gets increased. At the receiver, the effect of Z_k can be eliminated by performing modulus q operation on received data symbols.

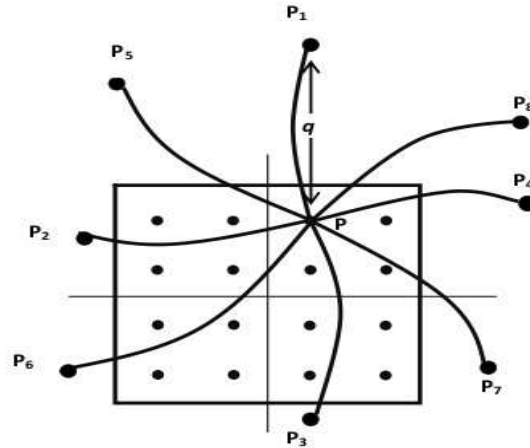


Figure 4.8 Expanded 16-QAM constellation for Tone Injection Technique
Tellado suggested to use a minimum value of $q = d\sqrt{M}$, where d is the minimum distance between two constellation points. The extended constellation points have spacing $q = \alpha d\sqrt{M}$, with $\alpha \geq 1$ to avoid BER performance degradation.

4.2.4 CODING SCHEME

An OFDM signal may result in a PAPR of order N , as discussed in section 3.2. Coding scheme can be used to reduce the PAPR of the OFDM signal. Consider a BPSK modulated OFDM system with N subcarriers and a coding scheme with code rate $1/2$. The code rate $1/2$ encoder converts N input bits to a block of $2N$ bits. Therefore, there are 2^{2N} possible combinations of $2N$ bit long code words, out of which 2^N code words with lowest PAPR are selected for transmission of N information bits. This scheme can effectively reduce the PAPR of the OFDM signal, but it requires an exhaustive search to find 2^N low PAPR code words out of 2^{2N} possible code words. For large number of subcarriers, it requires large memory blocks to store lookup table for encoding and decoding operations. It also results in data rate loss because for every N information bits, we have to transmit $2N$ number of encoded bits.

Example: Consider a BPSK modulated OFDM system with four subcarriers and code rate $3/4$

encoder. In this case there are 16 possible combinations of data blocks; and PAPR of each possible data block is calculated using (3.1), and its values are shown in Table 4.1.

It can be seen from Table 4.1 that four, four and eight combinations of data blocks have PAPR of 6.0dB, 3.7dB and 2.3dB respectively. Out of these 16 possible combinations, 8 combinations with 2.3 dB PAPR can be selected to map 3 bit binary information. In this scheme four subcarriers are required to transmit 3 bit binary information. Hence, it results in 25% data rate loss. This basic coding scheme has been extended and improved by many researchers e.g. use of complementary Golay codes by Popovic. However, the discussion of these methods is beyond the scope of this work.

Data Block	PAPR(dB)	Data Block	PAPR (dB)
1 1 1 1	6.0dB	-1 1 1 1	2.3dB
1 1 1 -1	2.3dB	-1 1 1 -1	3.7dB
1 1 -1 1	2.3dB	-1 1 -1 1	6.0dB
1 1 -1 -1	3.7dB	-1 1 -1 -1	2.3dB
1 -1 1 1	2.3dB	-1 -1 1 1	3.7dB
1 -1 1 -1	6.0dB	-1 -1 1 -1	2.3dB
1 -1 -1 1	3.7dB	-1 -1 -1 1	2.3dB
1 -1 -1 -1	2.3dB	-1 -1 -1 -1	6.0dB

Table 4.1:PAPR of all possible combinations of data block using coding scheme for PAPR reduction

CHAPTER 5

METHODOLOGY ADOPTED

The time domain OFDM signal has large envelope fluctuation therefore, PAPR of OFDM signal is very high. Thus HPAs with large linear range and high resolution ADCs/DACs are required to amplify OFDM signal and for its conversion between analog and digital domains respectively. We need to generate basic OFDM signal as our aim is to reduce PAPR of OFDM signal.

The code for OFDM generation and demodulation is in Appendix 1, Spectrum of OFDM Appendix 2, CDF of OFDM Appendix 3

The Techniques that we implemented to reduce PAPR:

Clipping:

It is a non-linear technique in which the reference signal (peak sequence) with which we compare our original signal is independent of input. It is simple and less expensive.

It has one disadvantage that we can't get the original signal through clipped signal exactly at the receiver so we get some error. This error is estimated by Minimum Mean Square Error (MMSE). It is an estimation method which minimizes the mean square error of the fitted values of dependent variable, which is a common measure of estimator quality. The matlab code for this technique is available in Appendix 4

Selected Mapping:

In this method, whole set of signal represent the same signal but from it most favorable signal is chosen related to PAPR transmitted. Side information must be transmitted with chosen signal. It is very reliable but main drawback that is side information must be transmitted along with chosen signal. The matlab code for this technique is available in Appendix 5

Tone Reservation:

This technique contains some set of reservation of tones. Reserved tones can be used to minimize the PAPR and used for multicarrier transmission. Depend on amount of complexity where there is number of tones is small reduction in PAPR may represent non negligible samples of available bandwidth. The advantage is that no process is needed at receiver end. The matlab code for this technique is available in Appendix 6

CHAPTER 6

SIMULATION RESULTS

6.1 Generation of OFDM signal & Spectrum:

Refer to Appendix1

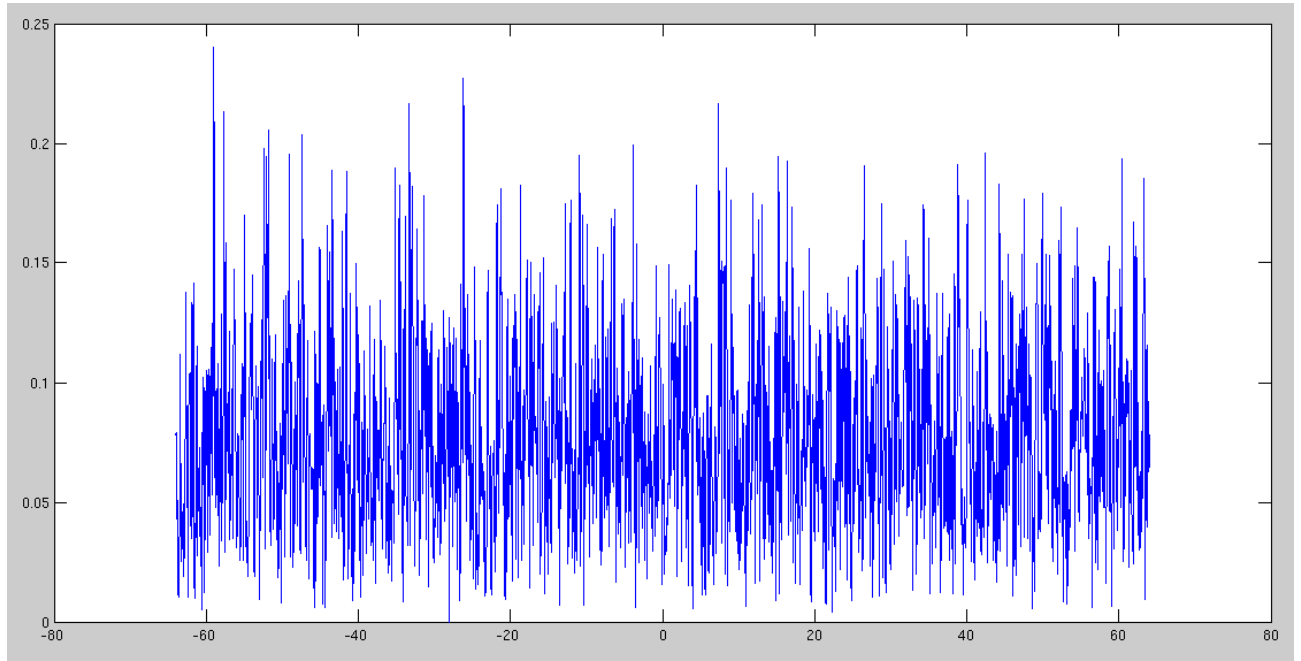


Figure 6.1: Result obtained from simulation of OFDM code

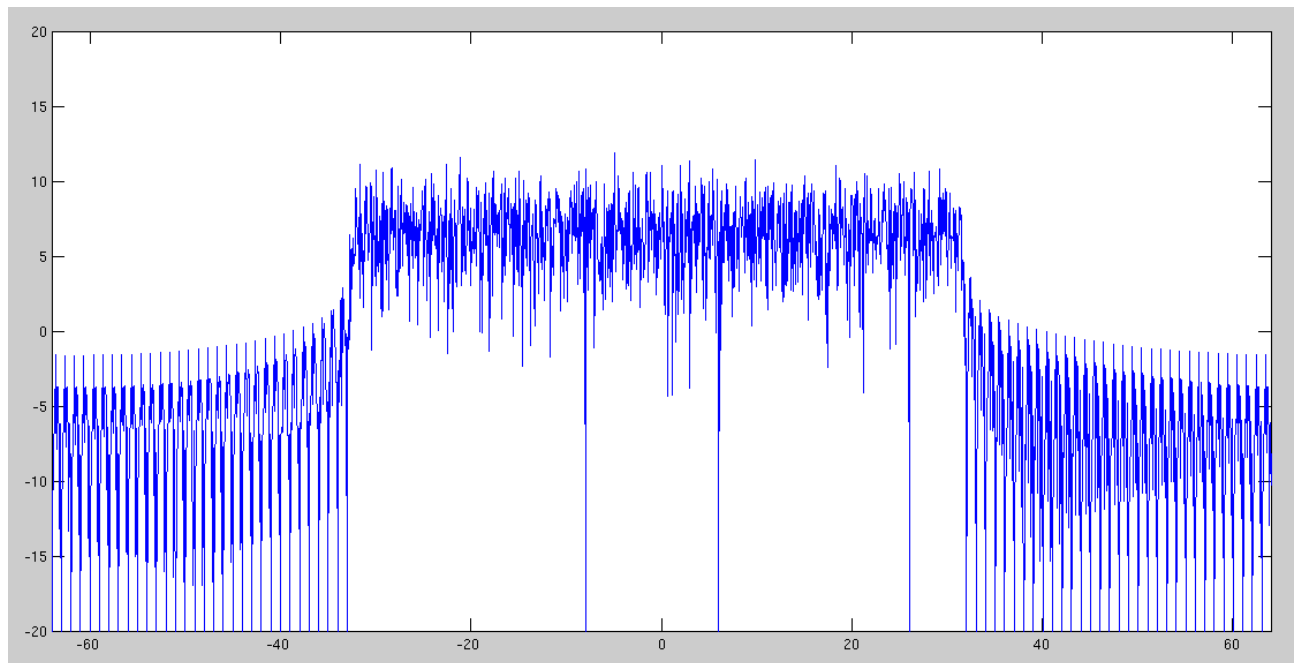


Figure 6.2: Spectrum of above OFDM signal

6.2 Cumulative Distribution Function (CDF):

Refer to Apendix2

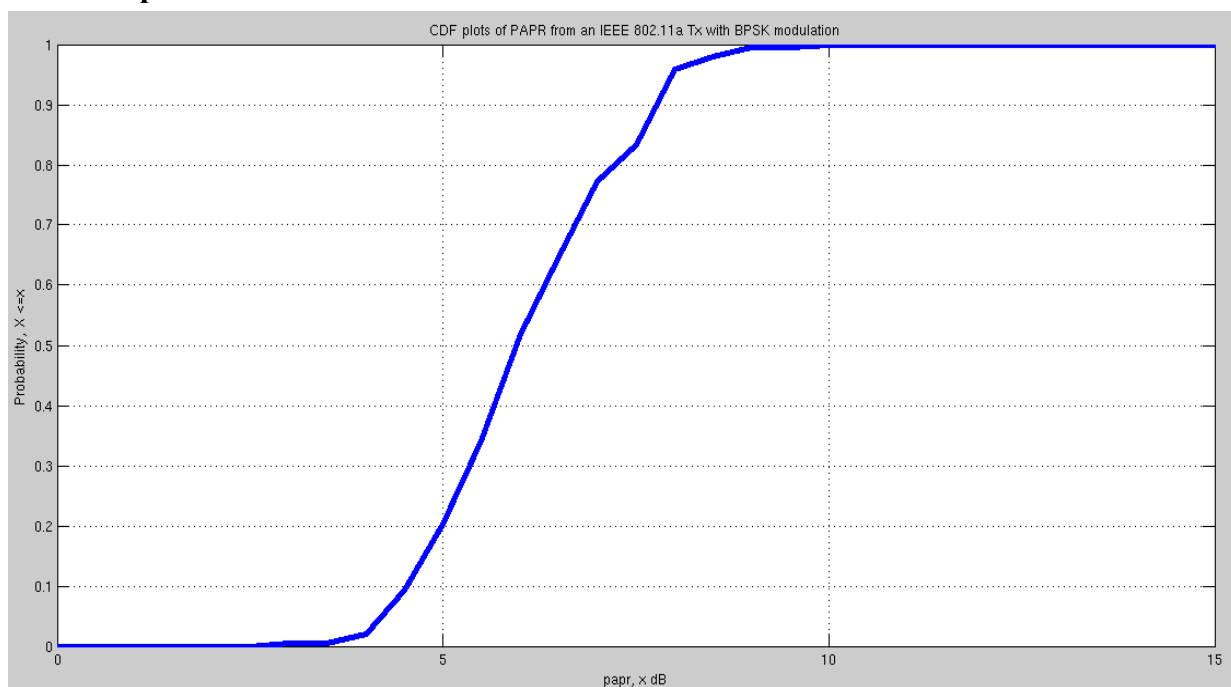


Figure 6.3: CDF graph obtained from Simulation

6.3 Clipping Technique:

Refer to Apendex3

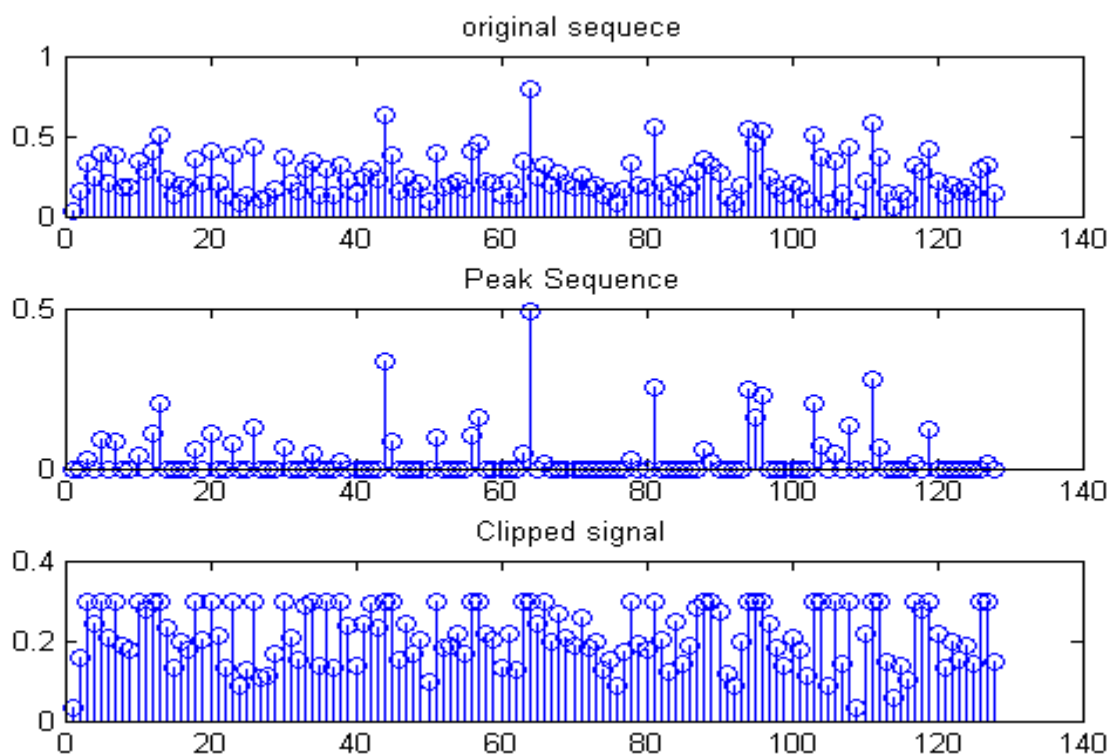


Figure 6.4: The result obtained by simulating Clipping Technique

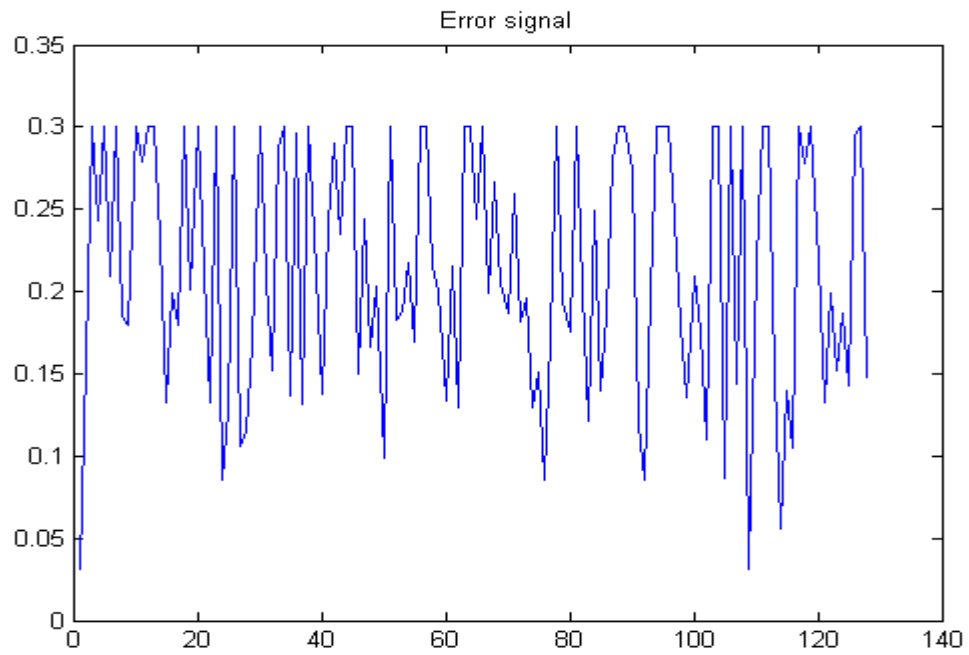


Figure 6.5: The error signal obtained in Clipping

PAPR of original signal in dB 20.6920

PAPR of Clipped signal 5.63dB

MMSE=0.0070

6.4 Slective Mapping (SLM) Technique:

Refer to Apendix4

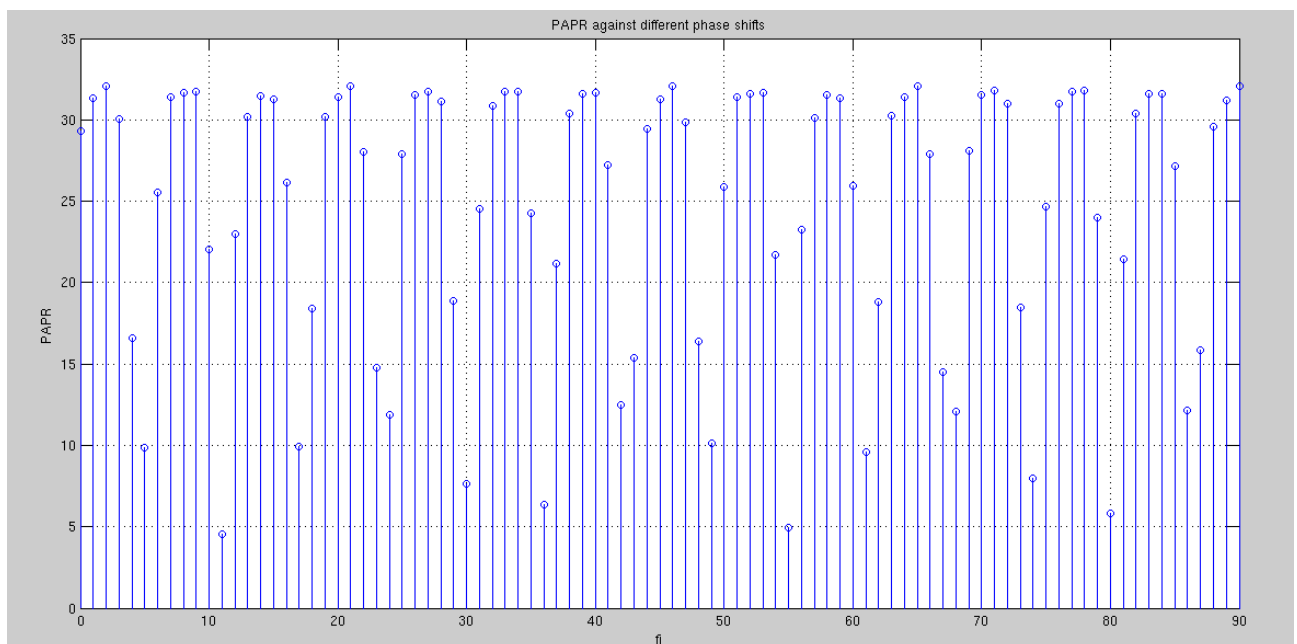


Figure 6.6: The result obtained by implementing SLM

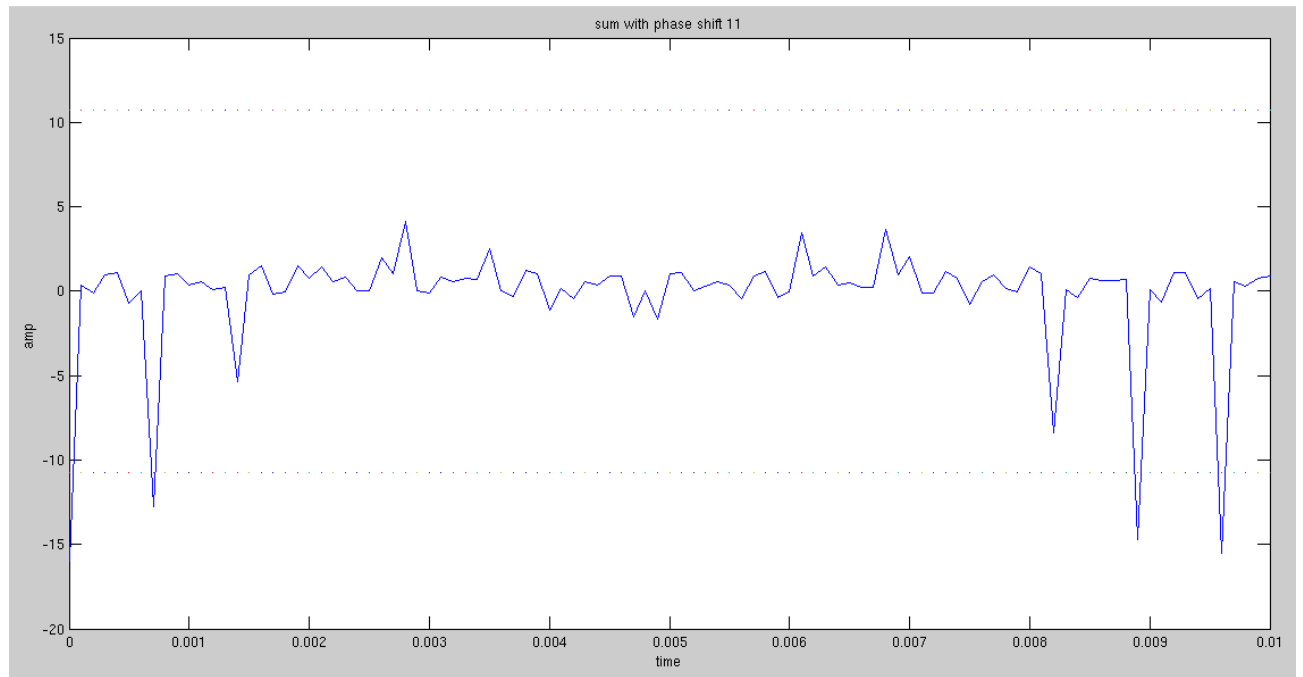
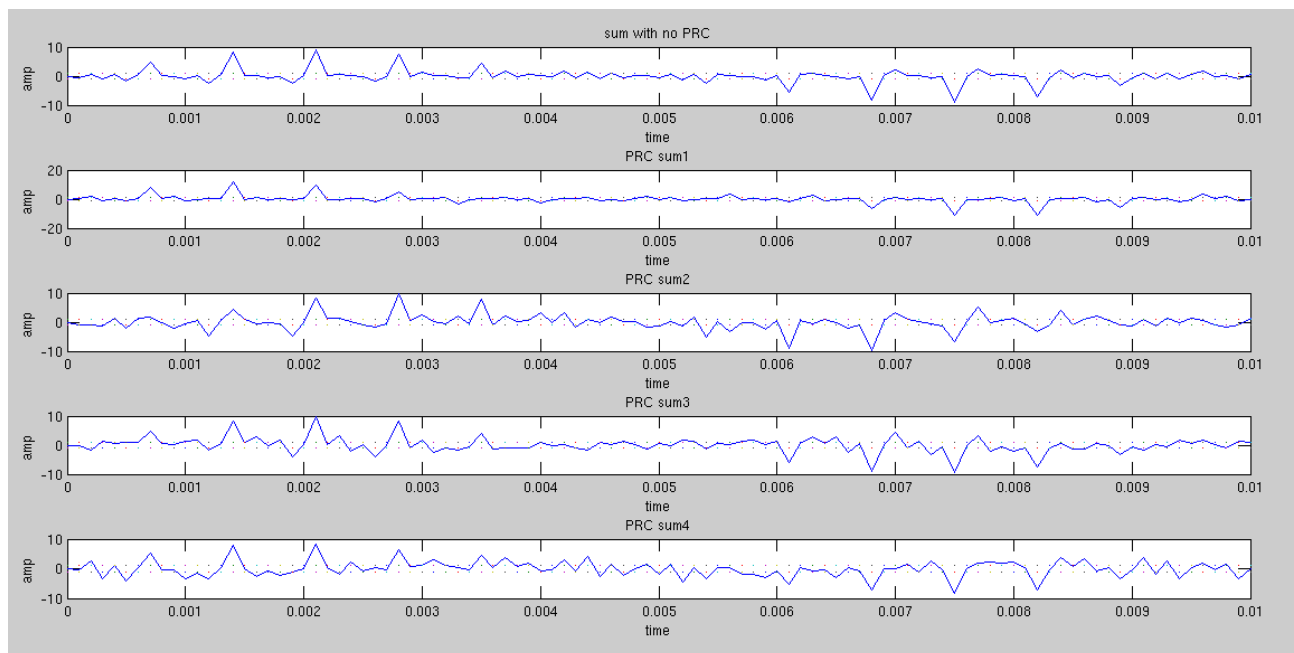


Figure 6.7: The ofdm signal with minimum PAPR

6.5 Tone Reservation:

Refer to Appendix5



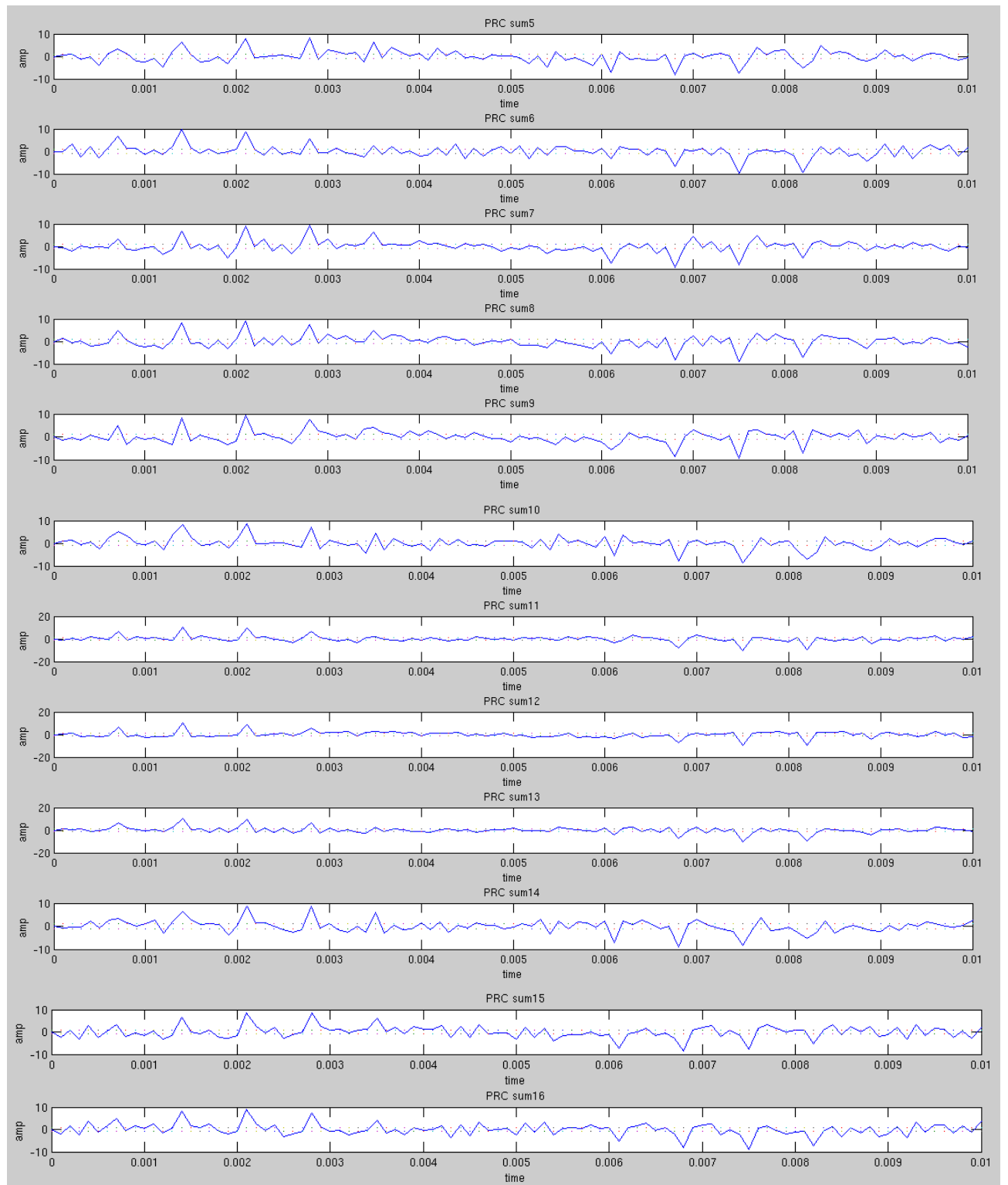


Figure 6.8: The result obtained by implementing tone reservation.

CHAPTER 7

CONCLUSIONS AND FUTURE WORK

Physical layer design is a very important aspect of any communication system and has a profound impact on the feasibility of communication processes at higher layers. Multicarrier systems are providing better in transmission than single carrier systems. It is evident that multi-carrier transmission is a very useful technique in combating the adverse effects of wireless channels and making use of the adversity to the benefit of the system. Future wireless applications will demand high data rate communication; this is not going to be an easy task, when dealing with the unpredictable wireless channel. The idea of multi-carrier transmission has emerged recently to be used for combating the hostile wireless channel and providing high data rate communications.

OFDM is a digital multi-carrier modulation method where a large number of closely spaced orthogonal sub-carriers are used to carry data. OFDM based transmission is a promising candidate to achieve high data rates via collective usage of a large number of subcarriers. Despite its several advantages, it suffers from two major disadvantages, which are high PAPR and ICI. Therefore, PAPR reduction and ICI cancellation are two major challenges in implementing an OFDM system. This thesis presents the study of existing PAPR reduction techniques. And we described several important aspects related to the PAPR & its overall effect on the OFDM system & give names several techniques adopted by the system according to the requirement. The PAPR depends on bandwidth efficiency. The PAPR as a function of the bandwidth efficiency behaves asymptotically almost identically for SC and OFDM, SC may have a high PAPR: a high PAPR is not unique to OFDM. It will appear whenever one is willing to have high bandwidth efficiency.

We have also aimed at investigating some of the techniques which are in common use to reduce the high PAPR of the system. Among the three techniques that we took up for study, we found out that Amplitude Clipping results in Data Loss, whereas, Selected Mapping (SLM) and Partial Transmit Sequence (PTS) do not affect the data. However, no specific PAPR reduction technique is the best solution for the OFDM system. Various parameters like loss in data rate, transmit signal power increase, BER increase, computational complexity increase should be taken into consideration before choosing the appropriate PAPR technique.

REFERENCE

- [1] Arun Gangwar, Manushree Bhardwaj An Overview: “*Peak to Average Power Ratio in OFDM system & its Effect*” International Journal of Communication and Computer Technologies, Vol 01-No.2, Issue:02 Sept 2012.
- [2] Ramjee Prasad, “*OFDM for Wireless Communications Systems*”, universal personal communications.
- [3] Ahmad R. S. Bahai, Burton R. Saltzberg, “*Multi-carrier digital communications Theory and applications of OFDM*”, Kluwer Academic / Plenum Publishers New York, Boston, Dordrecht, London, Moscow 1999.
- [4] Nicola Marchetti, Muhammad Imadur Rahman, Sanjay Kumar, Ramjee Prasad, Chapter2. “*OFDM: Principles and Challenges*”.
- [5] Dov Wulich, Lev Goldfeld, Gill R. Tsouri, “*Peak to Average Power Ratio in Digital Communications*”. IEEE Trans. pp 779-782.
- [6] Wu Y., W. Y. Zou, “*Orthogonal frequency division multiplexing: A multi-carrier modulation scheme*,” IEEE Transactions on Consumer Electronics, vol. 41, no. 3, pp. 392–399, Aug. 1995.
- [7] Van Nee R., Prasad R., “*OFDM for wireless Multimedia Communications*”, Artech House, 2003.
- [8] Chang R., Gibby R. “*A theoretical study of performance of an orthogonal multiplexing data transmission scheme*”, IEEE Transactions on Communication Technology, vol. 16, pp. 529-540, Aug. 1968.
- [9] Han S. H., Lee J. H., “*An overview of peak-to-average power ratio reduction techniques for multicarrier transmission*”, IEEE Wireless Communications, vol. 12, no. 2, April 2005, pp. 56-65.
- [10] Armstrong J., “*Peak-to-average power reduction for OFDM by repeated clipping and frequency domain filtering*”, Electronics Letters, vol. 38, no. 5, pp. 246–247, Feb. 2002.
- [11] Bäuml R. W., Fischer R. F. H., Hüber J. B., “*Reducing the peak-to average power ratio of multicarrier modulation by selective mapping*”, Electronics Letters, vol. 32, no. 22, pp. 2056–2057, Oct. 1996.
- [12] Cimini L. J., Sollenberger, N. R., “*Peak-to-Average Power Ratio Reduction of an OFDM Signal Using Partial Transmit Sequences*” IEEE Communications Letters, vol. 4, no. 3, pp. 86-88, March 2000.
- [13] Jayalath A. D. S., Tellambura C., “*SLM and PTS peak-power reduction of OFDM signals without side information*”, IEEE Transactions on Wireless Communications, vol. 4, no. 5, 2006–2013, Sept. 2005.

APPENDICES

Basic OFDM Code:

```
close all
clear all
clc

nbitpersym = 52; % number of bits per OFDM symbol(same as number of
                  subcarriers for BPSK)
nsym        = 10^4; % number of symbols
len_fft     = 64; % fft size
sub_car     = 52; % number of data subcarriers
EbNo        = 0:5:40;

EsNo= EbNo + 10*log10(52/64) + 10*log10(64/80); % symbol to noise ratio
snr= EsNo - 10*log10(64/80); % snr as to be used by awgn fn.

M = modem.pskmod(2); % modulation object

% Generating data
t_data=randint(nbitpersym*nsym,1);

% modulating data
mod_data = modulate(M,t_data);

% serial to parallel conversion
par_data = reshape(mod_data,nbitpersym,nsym).';

% pilot insertion
pilot_ins_data=[zeros(nsym,6) par_data(:,[1:nbitpersym/2]) zeros(nsym,1)
par_data(:,[nbitpersym/2+1:nbitpersym]) zeros(nsym,5)] ;

% fourier transform time doamain data and normalizing the data
IFFT_data = (64/sqrt(52))*ifft(fftshift(pilot_ins_data.')).';

% addition cyclic prefix
cyclic_add_data = [IFFT_data(:,[49:64]) IFFT_data].';

% parallel to serial coversion
ser_data = reshape(cyclic_add_data,80*nsym,1);

% passing thru channel
h=rayleighchan(1/10000,10);
changain1=filter(h,ones(nsym*80,1));
a=max(max(abs(changain1)));
```

```

changain1=changain1./a;
chan_data = changain1.*ser_data;

no_of_error=[];

ratio=[];

for ii=1:length(snr)

chan_awgn = awgn(chan_data,snr(ii),'measured'); % awgn addition

chan_awgn =a* chan_awgn./changain1; % assuming ideal channel estimation

ser_to_para = reshape(chan_awgn,80,nsym).'; % serial to parallel coversion

cyclic_pre_rem = ser_to_para(:,[17:80]); %cyclic prefix removal

FFT_recdata =(sqrt(52)/64)*fftshift(fft(cyclic_pre_rem.')).'; % freq
domain transform

% FFT_recdata = FFT_recdata./FFT_recdata1;

rem_pilot = FFT_recdata (:,[6+[1:nbitpersym/2] 7+
[nbitpersym/2+1:nbitpersym] 1]); %pilot removal

ser_data_1 = reshape(rem_pilot.',nbitpersym*nsym,1); % serial coversion

% ser_data_1 = ser_data_1./abs(FFT_recdata1);

z=modem.pskdemod(2); %demodulation object

demod_Data = demodulate(z,ser_data_1); %demodulating the data

[no_of_error(ii),ratio(ii)]=biterr(t_data,demod_Data) ; % error rate
calculation

end

% plotting the result

semilogy(EbNo,ratio,'--or','linewidth',2);
hold on;
EbN0Lin = 10.^(EbNo/10);
theoryBer = 0.5.*(1-sqrt(EbN0Lin./(EbN0Lin+1)));
semilogy(EbNo,theoryBer,'--ob','linewidth',2);
legend('simulated','theoritical')
grid on

xlabel('EbNo');
ylabel('BER')
title('Bit error probability curve for BPSK using OFDM');

```

Appendix 1

% OFDM signal and its spectrum (Guard Interval insertion)

clear all;

```
Fd=1;           % symbol rate (1Hz)
Fs=1*Fd;        % number of sample per symbol
M=4;            % kind(range) of symbol (0,1,2,3)

Ndata=1024;     % all transmitted data symbol
Sdata=64;       % 64 data symbol per frame to ifft
Slen=128;       % 128 length symbol for IFFT
Nsym=Ndata/Sdata; % number of frame -> Nsym frame
Gilen=144;      % symbol with GI insertion
GI=16;          % guard interval length
```

% vector initialization

```
X=zeros(Ndata,1);
Y1=zeros(Ndata,1);
Y2=zeros(Ndata,1);
Y3=zeros(Slen,1);
z0=zeros(Slen,1);
z1=zeros(Ndata/Sdata*Slen,1);
g=zeros(Gilen,1);
z2=zeros(Gilen*Nsym,1);
z3=zeros(Gilen*Nsym,1);
```

% random integer generation by M kinds

```
X = randint(Ndata, 1, M);
```

% digital symbol mapped as analog symbol

```
Y1 = modmap(X, Fd, Fs, 'qask', M);
```

% covert to complex number

```
Y2=amodce(Y1,1,'qam');
```

```
for j=1:Nsym;
```

```
    for i=1:Sdata;
        Y3(i+Slen/2-Sdata/2,1)=Y2(i+(j-1)*Sdata,1);
    end
```

```
    z0=ifft(Y3);
```

```
    for i=1:Slen;
        z1(((j-1)*Slen)+i)=z0(i,1);
    end
```

```
    for i=1:Slen;
        g(i+16)=z0(i,1);
    end
```

```
    for i=1:GI;
        g(i)=z0(i+Slen-GI,1);
    end
```

```
    for i=1:Gilen;
        z2(((j-1)*Gilen)+i)=g(i,1);
    end
```

```

        end

    end

% graph on time domain
figure(1);
f = linspace(-Sdata,Sdata,length(z1));
plot(f,abs(z1));

Y4 = fft(z1);

% if Y4 is under 0.01 Y4=0.001
for j=1:Ndata/Sdata*Slen;
if abs(Y4(j)) < 0.01
    Y4(j)=0.01;
end
end

Y4 = 10*log10(abs(Y4));

% graph on frequency domain
figure(2);
f = linspace(-Sdata,Sdata,length(Y4));
plot(f,Y4);
axis([-Slen/2 Slen/2 -20 20]);

```

Appendix 2

```

clear
nFFTSize = 64;
% for each symbol bits a1 to a52 are assigned to subcarrier
% index [-26 to -1 1 to 26]
subcarrierIndex = [-26:-1 1:26];
nBit = 10000;
ip = rand(1,nBit) > 0.5; % generating 1's and 0's
nBitPerSymbol = 52;

nSymbol = ceil(nBit/nBitPerSymbol);

% BPSK modulation
% bit0 --> -1
% bit1 --> +1
ipMod = 2*ip - 1;
ipMod = [ipMod zeros(1,nBitPerSymbol*nSymbol-nBit)];
ipMod = reshape(ipMod,nSymbol,nBitPerSymbol);

st = []; % empty vector

for ii = 1:nSymbol

    inputiFFT = zeros(1,nFFTSize);

    % assigning bits a1 to a52 to subcarriers [-26 to -1, 1 to 26]
    inputiFFT(subcarrierIndex+nFFTSize/2+1) = ipMod(ii,:);

    % shift subcarriers at indices [-26 to -1] to fft input indices [38 to 63]
    inputiFFT = fftshift(inputiFFT);

```

```

outputiFFT = 64*ifft(inputiFFT,nFFTSize);

% adding cyclic prefix of 16 samples
outputiFFT_with_CP = [outputiFFT(49:64) outputiFFT];

% computing the peak to average power ratio for each symbol
meanSquareValue = outputiFFT*outputiFFT'/length(outputiFFT);
peakValue = max(outputiFFT.*conj(outputiFFT));
paprSymbol(ii) = peakValue/meanSquareValue;

% concatenating the symbols to form the final output
st = [st outputiFFT_with_CP];

end

close all
paprSymboldB = 10*log10(paprSymbol);
[n x] = hist(paprSymboldB,[0:0.5:15]);
plot(x,cumsum(n)/nSymbol,'LineWidth',4)
xlabel('papr, x dB')
ylabel('Probability, X <=x')
title('CDF plot of PAPR Tx with BPSK modulation')
grid on

```

Appendix 3

```

clc;
clear all;
close all;
N=128;
x=randi(1,512);
M=16;
k=log2(M);
r=reshape(x,length(x)/k,k);
v=bi2de(r,'left-msb');
m=qammod(v,M);
y_if=ifft(m,N);
x=transpose(y_if);
x_abs=abs(x);
subplot(3,1,1);
stem(x_abs)
title('original sequece');
papr=10*log(max(x_abs.^2)/mean(x_abs.^2));
disp('PAPR of original signal in dB');
disp(papr);
t=0.3;
for i=1:1:N
if x_abs(i)>t

    x1(i)=x_abs(i)-t;
else
    x1(i)=0;
end
end
x3=abs(x1);

```

```

x4=x_abs-x3;

papr1=10*log(max(x4.^2)/mean(x4.^2));
disp('PAPR of clipped seq in dB');
disp(papr1);
subplot(3,1,2);
stem(x1)
title('Peak Sequence');
subplot(3,1,3);

stem(x4)
title('Clipped signal');

error=(abs(x_abs-x4)).^2;
MMSE=(sum(error))/N;
figure;
plot(x_abs-x1)
title('Error signal');
disp('MMSE=');
disp(MMSE);

```

Appendix 4

Code for Selective Mapping with Phase Rotations:

```

t=0:.0001:.01;
for fi=0:90
    x1=sin((2*180*100*t)+fi);
    x2=sin((2*180*200*t)+fi);
    x3=sin((2*180*300*t)+fi);
    x4=sin((2*180*400*t)+fi);
    x5=sin((2*180*500*t)+fi);
    x6=sin((2*180*600*t)+fi);
    x7=sin((2*180*700*t)+fi);
    x8=sin((2*180*800*t)+fi);
    x9=sin((2*180*900*t)+fi);
    x10=sin((2*180*1000*t)+fi);
    x11=sin((2*180*1100*t)+fi);
    x12=sin((2*180*1200*t)+fi);
    x13=sin((2*180*1300*t)+fi);
    x14=sin((2*180*1400*t)+fi);
    x15=sin((2*180*1500*t)+fi);
    x16=sin((2*180*1600*t)+fi);
    sum=x1+x2+x3+x4+x5+x6+x7+x8+x9+x10+x11+x12+x13+x14+x15+x16;
    peak=max(sum);
    avg=mean(sum.*sum);
    papr=10*log((peak^2/avg))

figure(1)
stem(fi,papr)
grid on; xlabel('fi'); ylabel('PAPR')
title('PAPR against different phase shifts')
hold on
end

%from the graph it's clear that 11 degrees is the optimum phase shift that
gives the least PAPR (4.5292 db)

```



```

x1a=sin((2*180*100*t)+11);
x2a=sin((2*180*200*t)+11);
x3a=sin((2*180*300*t)+11);
x4a=sin((2*180*400*t)+11);
x5a=sin((2*180*500*t)+11);
x6a=sin((2*180*600*t)+11);
x7a=sin((2*180*700*t)+11);
x8a=sin((2*180*800*t)+11);
x9a=sin((2*180*900*t)+11);
x10a=sin((2*180*1000*t)+11);
x11a=sin((2*180*1100*t)+11);
x12a=sin((2*180*1200*t)+11);
x13a=sin((2*180*1300*t)+11);
x14a=sin((2*180*1400*t)+11);
x15a=sin((2*180*1500*t)+11);
x16a=sin((2*180*1600*t)+11);
sum11=x1a+x2a+x3a+x4a+x5a+x6a+x7a+x8a+x9a+x10a+x11a+x12a+x13a+x14a+x15a+x16a;
avg11=mean(sum11.*sum11);
figure(2)
plot(t,sum11,t,avg11,t,-avg11)
xlabel('time'); ylabel('amp')
title('sum with phase shift 11')

```

Appendix 5

Code for Tone reservation:

```

t=0:.0001:.01;
g=1;
%these are the 12 information subcarriers (BPSK modulated)assuming all ones
x1=sin(2*180*100*t);
x2=sin(2*180*200*t);
x3=sin(2*180*300*t);
x4=sin(2*180*400*t);
x5=sin(2*180*500*t);
x6=sin(2*180*600*t);
x7=sin(2*180*700*t);
x8=sin(2*180*800*t);
x9=sin(2*180*900*t);
x10=sin(2*180*1000*t);
x11=sin(2*180*1100*t);
x12=sin(2*180*1200*t);
% these are the 4 reduction carriers we will map different combinations
% from them by changing the reduction subcarrier case (positive or negative)
r1=sin(2*180*1300*t);
r2=sin(2*180*1400*t);
r3=sin(2*180*1500*t);
r4=sin(2*180*1600*t);
%let us dedicate r1,r2,r3 and r4 as PRC or peak reduction carriers and
transmit on
%x1:x12 so when x1:x12 summation creates a peak, a combinatin from r1,r2,r3
and r4
%creates an antipeak but not the exact antipeak or the output would be a flat
signal from which data can be retreived

sum=x1+x2+x3+x4+x5+x6+x7+x8+x9+x10+x11+x12;
sum1=x1+x2+x3+x4+x5+x6+x7+x8+x9+x10+x11+x12+r1+r2+r3+r4;
sum2=x1+x2+x3+x4+x5+x6+x7+x8+x9+x10+x11+x12-r1-r2-r3-r4;

```

```

sum3=x1+x2+x3+x4+x5+x6+x7+x8+x9+x10+x11+x12+r1+r2-r3-r4;
sum4=x1+x2+x3+x4+x5+x6+x7+x8+x9+x10+x11+x12-r1-r2+r3+r4;
sum5=x1+x2+x3+x4+x5+x6+x7+x8+x9+x10+x11+x12-r1-r2-r3+r4;
sum6=x1+x2+x3+x4+x5+x6+x7+x8+x9+x10+x11+x12-r1+r2+r3+r4;
sum7=x1+x2+x3+x4+x5+x6+x7+x8+x9+x10+x11+x12+r1-r2-r3-r4;
sum8=x1+x2+x3+x4+x5+x6+x7+x8+x9+x10+x11+x12+r1-r2-r3+r4;
sum9=x1+x2+x3+x4+x5+x6+x7+x8+x9+x10+x11+x12+r1-r2+r3-r4;
sum10=x1+x2+x3+x4+x5+x6+x7+x8+x9+x10+x11+x12-r1+r2-r3+r4;
sum11=x1+x2+x3+x4+x5+x6+x7+x8+x9+x10+x11+x12+r1+r2+r3-r4;
sum12=x1+x2+x3+x4+x5+x6+x7+x8+x9+x10+x11+x12+r1-r2+r3+r4;
sum13=x1+x2+x3+x4+x5+x6+x7+x8+x9+x10+x11+x12+r1+r2-r3+r4;
sum14=x1+x2+x3+x4+x5+x6+x7+x8+x9+x10+x11+x12-r1+r2-r3-r4;
sum15=x1+x2+x3+x4+x5+x6+x7+x8+x9+x10+x11+x12-r1-r2+r3-r4;
sum16=x1+x2+x3+x4+x5+x6+x7+x8+x9+x10+x11+x12-r1+r2+r3-r4;

```

```

%calculating the PAPR

```

```

peak=max(sum);
avg=mean(sum.*sum);
papr=10*log((peak^2/avg))

```

```

peak1=max(sum1);
avg1=mean(sum1.*sum1);
papr1=10*log((peak1^2/avg1))

```

```

peak2=max(sum2);
avg2=mean(sum2.*sum2);
papr2=10*log((peak2^2/avg2))

```

```

peak3=max(sum3);
avg3=mean(sum3.*sum3);
papr3=10*log((peak3^2/avg3))

```

```

peak4=max(sum4);
avg4=mean(sum4.*sum4);
papr4=10*log((peak4^2/avg4))

```

```

peak5=max(sum5);
avg5=mean(sum5.*sum5);
papr5=10*log((peak5^2/avg5))

```

```

peak6=max(sum6);
avg6=mean(sum6.*sum6);
papr6=10*log((peak6^2/avg6))

```

```

peak7=max(sum7);
avg7=mean(sum7.*sum7);
papr7=10*log((peak7^2/avg7))

```

```

peak8=max(sum8);
avg8=mean(sum8.*sum8);
papr8=10*log((peak8^2/avg8))

```

```

peak9=max(sum9);
avg9=mean(sum9.*sum9);
papr9=10*log((peak9^2/avg9))

```

```

peak10=max(sum10);
avg10=mean(sum10.*sum10);
papr10=10*log((peak10^2/avg10))

```

```

peak11=max(sum11);
avg11=mean(sum11.*sum11);
papr11=10*log((peak11^2/avg11))

```

```

peak12=max(sum12);
avg12=mean(sum12.*sum12);
papr12=10*log((peak12^2/avg12))

```

```

peak13=max(sum13);
avg13=mean(sum13.*sum13);
papr13=10*log((peak13^2/avg13))

```

```

peak14=max(sum14);
avg14=mean(sum14.*sum14);
papr14=10*log((peak14^2/avg14))

```

```

peak15=max(sum15);
avg15=mean(sum15.*sum15);
papr15=10*log((peak15^2/avg15))

```

```

peak16=max(sum16);
avg16=mean(sum16.*sum16);
papr16=10*log((peak16^2/avg16))

```

```

%plotting
figure(1)
subplot (5,1,1)
plot(t,sum,t,g,t,-g)
title('sum with no PRC')
xlabel('time')
ylabel('amp')
subplot (5,1,2)
plot(t,sum1,t,g,t,-g)
title('PRC sum1')
xlabel('time')
ylabel('amp')
subplot (5,1,3)
plot(t,sum2,t,g,t,-g)
title('PRC sum2')
xlabel('time')
ylabel('amp')
subplot (5,1,4)
plot(t,sum3,t,g,t,-g)
title('PRC sum3')
xlabel('time')
ylabel('amp')
subplot (5,1,5)
plot(t,sum4,t,g,t,-g)
title('PRC sum4')
xlabel('time')
ylabel('amp')

```

```

figure(2)
subplot (5,1,1)
plot(t,sum5,t,g,t,-g)
title('PRC sum5')
xlabel('time')
ylabel('amp')
subplot (5,1,2)

```

```

plot(t,sum6,t,g,t,-g)
title('PRC sum6')
xlabel('time')
ylabel('amp')
subplot (5,1,3)
plot(t,sum7,t,g,t,-g)
title('PRC sum7')
xlabel('time')
ylabel('amp')
subplot (5,1,4)
plot(t,sum8,t,g,t,-g)
title('PRC sum8')
xlabel('time')
ylabel('amp')
subplot (5,1,5)
plot(t,sum9,t,g,t,-g)
title('PRC sum9')
xlabel('time')
ylabel('amp')

```

```

figure(3)
subplot (5,1,1)
plot(t,sum10,t,g,t,-g)
title('PRC sum10')
xlabel('time')
ylabel('amp')
subplot (5,1,2)
plot(t,sum11,t,g,t,-g)
title('PRC sum11')
xlabel('time')
ylabel('amp')
subplot (5,1,3)
plot(t,sum12,t,g,t,-g)
title('PRC sum12')
xlabel('time')
ylabel('amp')
subplot (5,1,4)
plot(t,sum13,t,g,t,-g)
title('PRC sum13')
xlabel('time')
ylabel('amp')
subplot (5,1,5)
plot(t,sum14,t,g,t,-g)
title('PRC sum14')
xlabel('time')
ylabel('amp')

```

```

figure(4)
subplot (2,1,1)
plot(t,sum15,t,g,t,-g)
title('PRC sum15')
xlabel('time')
ylabel('amp')
subplot (2,1,2)
plot(t,sum16,t,g,t,-g)
title('PRC sum16')
xlabel('time')
ylabel('amp')

```